

October 2019

THE CATALYTIC UREASE SUBUNIT UREC IS CRITICAL FOR BIFIDOBACTERIUM LONGUM UREA UTILIZATION

YANG LYU
University of Massachusetts Amherst

Follow this and additional works at: https://scholarworks.umass.edu/dissertations_2



Part of the [Biotechnology Commons](#), and the [Food Microbiology Commons](#)

Recommended Citation

LYU, YANG, "THE CATALYTIC UREASE SUBUNIT UREC IS CRITICAL FOR BIFIDOBACTERIUM LONGUM UREA UTILIZATION" (2019). *Doctoral Dissertations*. 1792.
https://scholarworks.umass.edu/dissertations_2/1792

This Open Access Dissertation is brought to you for free and open access by the Dissertations and Theses at ScholarWorks@UMass Amherst. It has been accepted for inclusion in Doctoral Dissertations by an authorized administrator of ScholarWorks@UMass Amherst. For more information, please contact scholarworks@library.umass.edu.

**THE CATALYTIC UREASE SUBUNIT UREC IS
CRITICAL FOR BIFIDOBACTERIUM LONGUM
UREA UTILIZATION**

A dissertation presented

by

YANG LYU

Submitted to the Graduate School of the
University of Massachusetts Amherst in partial fulfillment
of the requirements for the degree of

DOCTOR OF PHILOSOPHY

September 2019

The Department of Food Science

© Copyright by Yang Lyu 2019

All Rights Reserved

THE CATALYTIC UREASE SUBUNIT UREC IS CRITICAL FOR BIFIDOBACTERIUM LONGUM UREA UTILIZATION

A dissertation presented

by

YANG LYU

Approved by style and content by:

David A. Sela, Chair

Lili He, Member

Carrie-Ellen Briere, Member

Eric A. Decker, Department Head

Department of Food Science

DEDICATION

*I dedicate this thesis to
my beloved families and friends
for their constant support and unconditional love.*

ACKNOWLEDGEMENTS

First, I would like to thank my advisor, Dr. David A. Sela, for his acceptance to me into the lab, guiding me through my research and teaching me all the time. Without his encouragement, patience and trust, I would not accomplish so many challenges during My PhD study. I am very proud of being David's student and be part of the Sela Lab.

I would also like to thank my committee members, Dr. Lili He, Dr. Carrie- Ellen Briere, Dr. Yeonhwa Park and Dr. John Gibbons for their great support and guidance to my dissertation. I would also like to thank Dr. Margaret Stratton from Department of Biochemistry and Molecular Biology for her generous supports on my research projects, Dr, Doyle Ward from UMass Medical School for providing me valuable advice on the manuscript.

I would like to give many thanks to all my previous and present lab members, especially Ezgi Özcan, Xiaomeng You, Korin Albert, Asha Rani, Liv Dedon, Shuqi Li, Michelle Rozycki, Nate Howitz, Margaret Hilliard, Veronica Bedard, Alison Germagian, Li Tang, Timothy Yeung, Jonah Einson, for their precious friendship, support and encouragement. Many thanks to Cindy Kane for her support and help to me and other lab members. Furthermore, I will always appreciate the supports from all of Food Science faculties, staffs especially Fran Kostek, Deby Lee, David Prodanas, Stacy Apostolou and Mary Bell. Thanks to my roommates Min Gu, Mi Li, Changyin Dong, my department friend Victor Ryu for their precious friendship and encouragement.

In the end, I would like to thank my family, especially my mom and dad for their unconditional love, forever support on my decisions. Thanks to all the people that help me in my life.

ABSTRACT

THE CATALYTIC UREASE SUBUNIT UREC IS CRITICAL FOR BIFIDOBACTERIUM LONGUM UREA UTILIZATION

SEPTEMBER 2019

YANG LYU

B.S., CHINA AGRICULTURAL UNIVERSITY, CHINA

M.S., CHINA AGRICULTURAL UNIVERSITY, CHINA

PH.D., UNIVERSITY OF MASSACHUSETTS, AMHERST, MA

Directed by: Professor David A. Sela

In the first study, we investigated the utilization of a human milk nitrogen source, urea, by *Bifidobacterium*. Urea accounts for ~15% in human milk, which is an abundant non-protein nitrogen (NPN). Some bifidobacteria are found to harbor urease gene clusters that potentially enable their hydrolysis of the human milk urea. However, the underlying mechanisms are still unclear. To incisively link the urease gene cluster with bifidobacterial urea utilization, chemical mutagenesis (i.e. ethyl methanesulfonate) was performed on the urease-positive *Bifidobacterium longum* subsp. *suis* UMA399. Mutants were selected on differential media and genetic lesions were identified using whole genome sequencing. A mutant that did not exhibit urease activity, or utilize urea as a primary nitrogen source, was selected for further characterization. We found that a single-point mutation was located on the urease catalytic subunit *ureC* gene to prompt a substitution at residue 343 from glutamic acid to lysine (E343K). Recombinantly expressed and purified mutant UreC exhibits the loss of urease function. The mutation

was complemented by expressing the wild-type UreC in the mutated strain. The restoration of urease activity and urea utilization approached levels exhibited by the wild-type strain. Thus, UreC is essential for the bifidobacterial urea utilization phenotype.

In the ongoing research, we are exploring the ability of *Bifidobacterium* to utilize cysteine, a sulfur-containing proteinogenic amino acid. Previous studies have shown most *Bifidobacterium* cannot grow without cysteine (cysteine auxotrophic). It will be interesting to clarify why bifidobacteria cannot synthesize cysteine and how they assimilate cysteine from the gut environment as a necessity for propagation. Thus, we first evaluated bifidobacterial strains on their ability to grow on different sole nitrogen sources as well as sulfur sources. We found that only *B. boum* LMG10736 was able to grow in methionine as a sole nitrogen source, the rest of the strains are all cysteine auxotroph. However, *B. boum* LMG10736 was not able to utilize sulfate and sulfide for its growth. We therefore proposed that the methionine degradation pathway may be silenced under the transcriptional or translational regulations.

TABLE OF CONTENTS

	Page
ACKNOWLEDGEMENTS.....	v
ABSTRACT.....	vii
LIST OF TABLES.....	xiii
LIST OF FIGURES.....	xiv
CHAPTER	
1. INTRODUCTION.....	1
2. LITERATURE REVIEW.....	4
2.1 Introduction.....	4
2.2 Current barriers for developing genetic tools for <i>Bifidobacterium</i>	4
2.3 Transformation.....	5
2.4 Heterologous gene expression in <i>Bifidobacterium</i>	8
2.5 Mutagenesis systems in <i>Bifidobacterium</i>	10
2.5.1 Targeted mutagenesis.....	10
2.5.2 Random mutagenesis.....	11
2.6 Future Perspectives.....	12
3. THE CATALYTIC UREASE SUBUNIT UREC IS CRITICAL FOR <i>BIFIDOBACTERIUM LONGUM</i> UREA UTILIZATION.....	15
3.1 Introduction.....	16
3.2 Material and Methods.....	18
3.2.1 Bacterial Strains and Culture Conditions.....	18

3.2.2 Mutant generation by Ethyl methane sulfonate (EMS)	18
3.2.3 Genome Sequencing and SNP Analysis	19
3.2.4 Microplate Growth Assay	19
3.2.5 Determination of Urease Activity	20
3.2.6 The Construction of the UreC expression Vector	21
3.2.7 Purification of UreC and In Vitro Urease Activity	22
3.2.8 Differential Scanning fluorimetry (DSF)	23
3.2.9 Construction of the UreC expression Shuttle Vector	24
3.2.10 Electroporation and Plasmid Isolation from the Mutant	24
3.2.11 Statistical Analysis	25
3.2.12 Protein Structure Stability Prediction	26
3.2.13 Phylogenetic Analysis	26
3.3 Results	26
3.3.1 Urease activity is strain-dependent and is elevated by urea and Ni ²⁺	26
3.3.2 A urease-deficient mutant from <i>B. suis</i> UMA399 was selected and identified	30
3.3.3 EMS mutagenesis resulted in a nonsynonymous mutation on the mutant <i>ureC</i> gene	31
3.3.4 Purified wild-type UreC restored urease activity after incubation with mutant lysates	34
3.3.5 Purified mutant UreC is different in confirmation vs. WT UreC	35
3.3.6 Transformation of pDOJ-U into the mutant complement urease activity ...	36

3.4 Discussion.....	39
3.5 Conclusions.....	42
3.6 Acknowledgements.....	43
3.7 Author contributions	43
4. EXPLORING L-CYSTEINE AUXOTROPHY IN BIFIDOBACTERIUM.....	44
4.1 Introduction.....	44
4.2 Material and Methods	45
4.2.1 Bacteria and Culture Conditions	45
4.2.2 Construction of the CysK and MetB Expression Vector	46
4.2.3 Electroporation.....	46
4.2.4 Growth Dependence on Nitrogen and Sulfur Source	47
4.2.5 Mutant generation by Ethyl methane sulfonate (EMS)	48
4.2.4 Multiple Sequence Alignment	48
4.2.5 Distribution of cysteine and methionine biosynthesis genes in <i>Bifidobacterium</i>	48
4.2.6 Statistical Analysis.....	49
4.3 Results.....	49
4.3.1 UMA272, UMA399 and JCM12489 are cysteine auxotrophic strains.....	49
4.3.2 Truncated CysK and MetB in UMA272 is not responsible for cysteine auxotrophy	50
4.3.3 LMG10736 is a cysteine prototroph	52

4.3.4 LMG10736 can utilize methionine as both nitrogen and sulfur source but cannot utilize <i>in vitro</i> sulfate or sulfide as sulfur source.	54
4.3.5 Predicted cysteine biosynthesis pathways in bifidobacterial strains.....	57
4.4 Discussion.....	58
4.5 Conclusions.....	59
5. FUTURE WORK.....	61
APPENDIX:SUPPLEMENTARY TABLES AND FIGURES.....	63
BIBLIOGRAPHY.....	68

LIST OF TABLES

Table	Page
1 Prediction of wild-type UreC stability changes upon the single-point mutation by STRUM.....	34
2 Electro-transformation efficiency.....	37

LIST OF FIGURES

Figure	Page
1 The Plasmid Artificial Modification (PAM) strategy applied in <i>Bifidobacterium</i>	8
2 Maximum likelihood phylogenetic analysis of the bifidobacterial UreC protein.....	28
3 Urease activity among multiple bifidobacterial strains cultured from complex nitrogen.	29
4 Urease activity among multiple bifidobacterial strains cultured from complex nitrogen.	30
5 Urease activity (A) and growth ability of the mutant strain in 2% urea as a primary nitrogen source (B).	31
6 Urease gene cluster of <i>B. suis</i> UMA399 and <i>B. infantis</i> UMA272 (A) and Distribution of urease genes on variant bifidobacterial genomes (B).....	33
7 Urease activity was restored by purified UreC.....	35
8 Configuration change of the wild-type UreC and mutant UreC detected by differential scanning fluorimetry.	36
9 Construction of the UreC expression shuttle vector pDOJ-U.....	37
10 Urease activity was complemented by expressing the wild-type <i>ureC</i> gene in the mutant.	38
11 Growth phenotype complemented by pDOJ-U.....	39
12 Growth phenotype of <i>B. infantis</i> UMA272, <i>B. suis</i> UMA399 and <i>B. scardovii</i> JCM12489 in cysteine and methionine and urea.	50
13 Multiple alignment of cystathionine beta-synthase (EC 4.2.1.22) protein sequence in variant species of <i>Bifidobacterium</i>	51
14 Growth phenotype of <i>B. infantis</i> UMA272 with or without pDOJ-cysK-metB in cysteine and methionine.....	52
15 Growth phenotype of <i>B. boum</i> LMG 10736 in L-cysteine, methionine and glutamine.....	53
16 Growth phenotype of <i>B. boum</i> LMG 10736 in modified medium that contained sulfur containing amino acids or sulfide.....	55
17 Predicted pathways of cysteine and methionine biosynthesis in <i>Bifidobacterium</i>	56

18 Distribution of cysteine and methionine biosynthesis genes in *B. infantis* UMA272 (ATCC15697), *B. suis* UMA399, *B. boum* LMG10736, *B. scardovii* JC12489.57

CHAPTER 1

INTRODUCTION

The human gut microbiome is a complex system consists of diverse microbial commensals, accounting for 10^{13-14} cells in the human gastrointestinal (GI) tract [1]. Over 1000 gut bacterial species have been characterized, from which most abundant bacterial phyla are *Bacteroides*, *Firmicutes*, *Proteobacteria* and *Actinobacteria* [2]. Numerous studies have found that turbulence in human gut microbiota is associated with many diseases such as diabetes [3], obesity [4], irritable bowel syndrome (IBS) [5], autoimmune disease [6], allergy [7], cancer [8], even brain disease [9]. It is well established that a healthy gut flora is responsible for overall health of the host [10]. The human gut microbiota is known as a dynamic and evolutionary system associated with host diversity (e.g., age and genetic identity) and environmental factors (e.g., living habits and geographic variations)

The colonization of intestinal bacteria begins in fetus and the infant gut microbiota is established after birth. The early establishment of gut microbiota can be affected by delivery mode (vaginal vs. caesarean section) [1]. The feeding mode, including exclusively breastfeeding and formula feeding during the first 6 months postpartum to 2 years of life will have profound effects on infant health and development [11]. Certain human milk nutrients can selectively enrich beneficial microbes in the infant microbiota, such as *Bifidobacterium* enriched by the human milk oligosaccharides (HMOs). While HMOs maintain the predominance of certain infant gut microbial cohorts, the access of nitrogen sources to the lower infant gut is unclear. Compared to bovine milk, human milk contains less protein but more non-protein nitrogen (NPN) [12]. The non-protein nitrogen compounds, including urea, uric acid,

creatine, peptides, amino acids, nucleotides comprise ~25% of human milk nitrogen [13]. The bioactive functions of these NPN compounds has not been well studied.

Our **long-term goal** is to investigate the interactions between human milk molecules and the microbes that colonize the infant gut. We are seeking answers of how human milk drives the establishment of the infant gut microbiome early in life and how it contributes to infant health. The **specific objective** of this thesis work is to study how the infant gut beneficial microbe, *Bifidobacterium* utilizes the human non-protein nitrogen, Urea, via the function of their urease gene cluster. Our **central hypothesis** is that human milk urea can be salvaged through bifidobacterial urease activity in the infant gut and potentially provide a secondary nitrogen reservoir to the infant host. We will test our hypothesis following the four **specific aims**:

Specific aim 1: Genomic analysis of the bifidobacterial urease gene cluster and detecting urease activity in Bifidobacterium

Sequenced genomes in *Bifidobacterium* will be checked for presence or absence of the urease genes. Multiple sequence alignment (MSA) will be performed on each gene of urease gene cluster among variant (sub) species of *Bifidobacterium*, followed by phylogenetic analyses. The configuration of a complete bifidobacterial urease gene cluster will be visualized. A developed quantitative urease assay will be used to detect urease activity in multiple bifidobacterial strains. The impact of substrate-Urea and cofactor-Nickel on urease activity will also tested.

Specific aim 2: Developing a bifidobacterial urease mutant and the phenotypic analysis of the mutant strain.

Bifidobacterium longum subsp. *suis* UMA399 will be treated with ethyl methane sulfonate (EMS). Mutants generated from EMS mutagenesis and will be selected from a developed differential agar, accompanied by phenotypic analyses. SNPs (Single

Nucleotide Polymorphisms) and relative mutations will be identified by whole genome sequencing and SNP-Calling. The mutant phenotype will be analyzed by both urease assay and growth assay using urea as a primary nitrogen source. To study the protein level deficiency of the mutant urease, the mutant urease will be overexpressed in *E. coli* using the SUMO fusion system followed by biochemical characterization. To complement the mutation, wild-type genes will be expressed on an *E. coli*-*Bifidobacterium* shuttle vector inside the mutant cells.

Specific aim 3: Developing genetic tools for Bifidobacterium longum subspecies strains

An electro-transformation system that allows the transferring of multiple *E. coli*-*Bifidobacterium* shuttle vectors into *Bifidobacterium longum* subspecies strains will be established via optimization of the electroporation method, including electroporation wash buffers, intensity of electric pulse.

Specific aim 4: Exploring the cysteine auxotrophic behavior in Bifidobacterium and initially predicting an underlying mechanism

Bifidobacterial strains from variant (sub) species will be tested on their growth ability in different sole nitrogen sources, to check if they are cysteine auxotroph or prototroph. To test if cysteine synthetic genes are silenced in the cysteine auxotrophic strains, chemical mutagenesis will be performed on these strains and to select mutants that turned to cysteine prototroph. Sequenced Bifidobacterial genomes will be checked for presence or absence of the cysteine biosynthetic pathway genes to provide an initial hypothesis for cysteine auxotrophic behavior in *Bifidobacterium*.

CHAPTER 2

LITERATURE REVIEW

2.1 Introduction

Bifidobacterium, a major of human gut colonizer, have been widely reported for their health benefits on human body such as improving immunity, reducing irritable bowel syndrome (IBS), and lowering cholesterol [14-17]. Some bifidobacterial species have been added to probiotic food or pharmaceuticals due to their beneficial effects. Over the past decade, the knowledge on interactions of *Bifidobacterium* with variant hosts and other gut members as well as their probiotic functions has been enhanced by cutting-edge techniques (genome, transcriptome, proteome or metabolome analysis). It is then important to deeply clarify the mechanisms behind those beneficial impacts. To confirm that specific genes identified by omics data are essential for a pathway, gene modification techniques such as knockout and gene overexpression are required. However, compared to many other bacteria, gene modification systems have not been established for the genus *Bifidobacterium* until recently. In this review, the barriers for establishing gene modification systems as well as the current genetic tools available for bifidobacteria will be comprehensively introduced.

2.2 Current barriers for developing genetic tools for *Bifidobacterium*

So far, several factors have been differentiated *Bifidobacterium* from other bacteria regarding their low ability to take up and maintain outer DNAs. The first is the thick cell wall of bifidobacteria. The multi-layers of peptidoglycan are proposed to hinder the intake of exogenous DNA as the first barrier. The second factor is the environmental stress such as oxygen that are toxic to bifidobacteria as they are general anaerobes. The major factor that impede the developing of genetic tools for

Bifidobacterium is the intracellular restriction/modification (R-M) systems. The R-M system is a widely distributed protective mechanisms in prokaryotes against invading DNAs such as phages. It comprises of a restriction endonuclease (REase) and cognate methyltransferase (MTase) [18, 19] and can be classified into four groups (type I, II, III and IV) [20]. In a type II R-M system, the bifidobacteria self-DNA is protected by MTase methylation that modifies cytosyl or adenosyl residues within the DNA [21, 22]. These DNA loci is also recognized by the corresponding REase, but due to methylation, REase will not cut self-DNA. In contrast, outer DNAs without methylation will be recognized and cut by REase, which explains why exogenous DNA such as plasmids are not stable in bifidobacteria. The distribution of the four R-M systems in bifidobacteria is pretty strain-dependent and can be analyzed by REBASE (<http://rebase.neb.com/rebase>) with known genome sequence [23]. Bifidobacterial strains with more R-M systems are potentially more difficult to take up exogenous DNAs compared to those with less R-M systems.

2.3 Transformation

Transformation is the process when competent bacteria are able to take up foreign DNA into their cells. For bifidobacteria, electro-transformation or electroporation is the most used method. During electroporation, an electric pulse is applied and will create pores on the cell membrane. Negatively charged DNA like plasmids or vectors get into the cells accordingly. The transformation of designed vectors for overexpression or mutagenesis of specific genes are fundamental and essential to study the beneficial effects of bifidobacteria. However, the application of transformation is limited to various bifidobacterial species or strains. A major cause is the presence of R-M systems which degrades foreign DNA imported into the cells. So far, there has been many reports on certain bifidobacterial strains transformed with

different *E. coli*-*Bifidobacterium* shuttle vectors [24-29]. Most shuttle vectors are created by adding the *E. coli* replicons and antibiotic resistant markers to the backbone of a bifidobacterial-originated plasmid which has been reviewed by Sun *et. al* [30]. Current transformation methodology for bifidobacteria has been advanced based on previous studies during the past decades reviewed by Gulielmetti *et. al* [31]. Right now, the conditions for making competent cells tends to be similar among various species. Key experimental conditions include a prerequisite anaerobic environment, high concentrations of sugars (sucrose, raffinose, fructo-oligosaccharides etc.) added into the growth medium [24, 26, 29, 32], the using of mid-logarithmic-phase cells ($OD_{600\text{ nm}} = 0.4 - 0.6$) as well as a washing buffer containing high-amount sucrose (0.5 M), and a 30 min preincubation before the electric pulse (25 μF , 200 Ω , 2.2 kV) are widely used in most recent studies on bifidobacteria. In a recent study that transformed pBES2 into *B. bifidum*, the use of 0.2 M NaCl as the cell wall weakening agent resulted in a 20-fold increase in the efficiency [33]. Still, for unreported bifidobacterial species, an optimization on the methodology is strongly recommended as strain/species-variance is quite normal [31], The optimization includes conditions for making competent cell, the amount of plasmid DNA used, as well as the electric pulse intensity. The median transformation efficiency is 10^3 CFU per μg plasmid DNA by electroporation [34]. For targeted mutagenesis using the vector for homologous recombination, the efficiency is suggested to be above 10^5 CFU per μg plasmid DNA. Besides optimized transformation conditions, plasmid artificial modification (PAM) on the vectors by the host bifidobacterial methyltransferase genes has been found to improve their stability against the R-M systems [27, 28, 35, 36] (**Figure 1**). In this strategy, the plasmid vectors are propagated inside an *E. coli* expressing the methyltransferase from the target bifidobacterial strain before introduced to the bifidobacterial cells. As vectors are

modified, they are less recognized by the nuclease from the R-M systems and are more stable inside the cell. In recent years, the use of single-molecule real-time (SMRT) DNA sequencing enables a more accurate and comprehensive analysis on all the recognition sequences of methyltransferases and the methylation site. This will further facilitate the application of the PAM method and more likely increase the efficiency of electro-transformation of interested *Bifidobacterium* in the future.

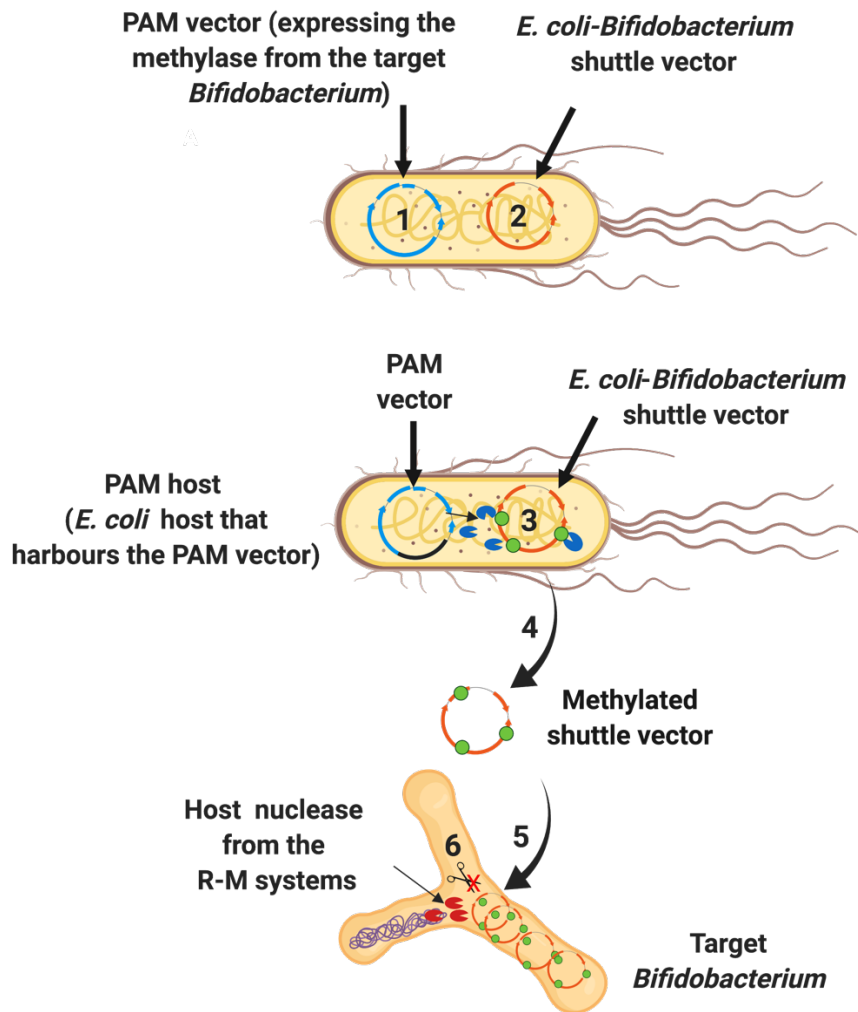


Figure 1 The Plasmid Artificial Modification (PAM) strategy applied in *Bifidobacterium*.

(1) Introduction of a PAM vector that expresses methylase from the target bifidobacterial strain. (2) Introduction of the *E. coli-Bifidobacterium* shuttle vector into the PAM host. (3) The shuttle vector is modified by methylase on the recognition sites. (4) Extraction of the shuttle vectors from the PAM host. (5) Electro-transformation of the shuttle vector into the target bifidobacterial cells. (6) The methylated shuttle vector is protected from the nuclease cleavage and can propagate in the cells.

2.4 Heterologous gene expression in *Bifidobacterium*

So far, heterologous gene expression has been used for identifying the gene functions of bifidobacteria, as well as using bifidobacteria as the carriers for expressing

useful enzymes. Currently, antigen or prodrug-converting molecules have been expressed in *Bifidobacterium* in order to use them as a live vaccine or for cancer therapy. Thus, it is very important to establish a sophisticated heterologous gene expression system for various experimental purposes. The major factors to consider for gene expression modulation in bifidobacteria are promoter and the ribosome-binding-site (RBS).

The promoter initiates the transcription of a gene by recruiting the RNA polymerase and controls the gene expression. In bacteria, promoters are consisted by a region from -35 sequence to a -10-sequence upstream transcription start site of the gene. Promoter activity is a critical factor for heterologous gene expression, the low or high activity of the chosen promoter is dependent on the purpose of the study. The overexpression of an exogenous gene might be toxic to the host cells; while a strict inducible promoter enables the control of its expressed genes. The activity of promoters in bifidobacteria has been analyzed in many studies reviewed by [30], via the promoter-reporter assay [37]. The reporter genes so far used include the green fluorescent protein, beta-glucuronidase (*gusA*), and luciferase. In particularly, the luciferase reporter system is applicable to measure the promoter activity *in vivo* [38]. The constitutive promoters *gap* (P_{gap}) and *hup* (P_{hug}) has shown high activities in bifidobacteria [39]. Inducible promoters, such as the arabinose inducible promoter P_{BAD} [40] and a bile-induced promoter P_{Bile} [41] has been used for controlled gene expression in bifidobacteria. For bifidobacteria that are not able to utilize arabinose, P_{BAD} will not be suitable.

The translational regulation is also an important factor to consider when performing heterologous gene expression, in this case ribosome-binding-site (RBS). RBS is usually optimized for translation initiation efficiency of a target gene. In *Bifidobacterium*, the length of the RBS as well as its distance to the start codon will

both influence the gene expression [42]. An optimal RBS has been identified *B. longum* 105-A, with the sequence (5'-AAGGAG-3') [43], which is quite different from the RBS conserved in *E. coli* (5'-AAGGAG-3'). The optimal distance to the start codon is suggested to be 5 bp. So far, limited knowledge is known about the translational regulation in *Bifidobacterium*. Future efforts are significant to elucidate both the transcriptional and translational impact on the gene expression in *Bifidobacterium* that can support their future application as gene-manipulated drug carrier in pharmaceuticals.

2.5 Mutagenesis systems in *Bifidobacterium*

2.5.1 Targeted mutagenesis

The most direct way to study gene function is by reverse genetics. Reverse genetic tools include directed gene knockout, gene silencing, and transgene interference. In many bacteria, targeted gene knockout via homologous recombination has been frequently used [44]. In bifidobacteria, the currently utilized targeted gene mutagenesis system is homologous recombination [44]. During homologous recombination, designed non-replicating plasmids with two homology arms on each side flanking the desired mutation or insertion. Target gene is split during single-crossover or double-crossover of the plasmid internal region and the chromosomal target gene. Even though this technique is quite established in other gram-positive bacteria such as *Lactobacillus*, it is very difficult to perform in *Bifidobacterium* until currently. The reason is still attributed to the R-M systems that prevent the introduction of the vectors for homologous recombination [45]. To date, only a few targeted gene knockout tools are available for certain bifidobacterial species including *B. longum* NCC2705 and *B. breve* UCC2003 by combining the plasmid artificial modifications (PAM) with a homologous recombination system as mentioned previously [45, 46]. The shuttle vector, in this case

designed for homologous recombination is propagated inside the *E. coli* PAM host expressing the methylase from *Bifidobacterium* of interest. Vectors are therefore modified by methylation before entering bifidobacterial cells for recombination. As modified shuttle vectors is to some extent protected from the endonuclease of the R-M systems, it is more stable. Therefore, there will be more opportunities to have the vector cross-over or recombination with the target gene loci on the chromosome. However, the PAM-based methods are strongly strain-dependent and limited for most bifidobacteria. So far, this technique has only been successful in *B. longum* NCC2705 [46, 47], *B. longum* 105-A [46, 48], *B. longum* 35624 [36], *B. longum* NCIMB8809 [49], *B. lactis* NCC2818 [50], *B. lactis* DSM10140 [51], *B. breve* UCC2003 [16, 52-56], *B. breve* BR-A29 [57], *B. breve* JCM7017 [58, 59] and *B. breve* NCFB2258 [52]. As for homologous recombination by using *Bifidobacterium* strains, a relatively high transformation efficiency of over 10^4 CFU per μg DNA is demonstrated. Thus, for strains with low transformation efficiency, this system is not applicable. Future efforts toward the development of broad-range targeted gene mutagenesis techniques are still of great demand.

2.5.2 Random mutagenesis

Forward genetics is another way to identify sequence variations responsible for a given phenotype of an organism. Different from reverse genetics that causes known sequence changes, this approach identifies the mutant phenotype from random mutagenesis or natural spontaneous mutation [60]. The mutant is selected with the phenotype of interest, followed by the mapping of gene mutations throughout the chromosomes. Random mutagenesis can be introduced by chemical mutagens or by UV [61]. One of the frequently used chemical mutagen is ethyl methane sulfonate

(EMS). EMS can cause base-pair transitions from C/G-to-A/T on the target genome, resulting in random loss of functions in the mutants [62]. As mentioned previously, tools for targeted mutagenesis for *Bifidobacterium* are very limited. The development of reverse genetic tools is time-consuming as well. However, chemical mutagenesis provides a convenient way to generate mutants from *Bifidobacterium*. EMS has been extensively used in various organisms, including prokaryotes and eukaryotes. Particularly, it has been applied to *B. breve* and *B. longum* strains to select mutants [63, 64].

Besides chemical mutagenesis, a Tn5-based transposon mutagenesis system has been applied to *Bifidobacterium breve* UCC2003 and *Bifidobacterium breve* NCFB2258 [65]. A transposon is a DNA sequence that can be able to move within a genome, sometimes creating or reversing mutations on the bacterial genome [66]. Using transposon mutagenesis, a mutant library with genome-wide transposon-insertion mutations can be created followed by phenotypic screenings for desired phenotype [67]. However, this experiment also needs plasmids transferred into the bifidobacterial strain, which requires transformation efficiency. Therefore, the application of chemical mutagenesis maybe a better tool for creating random mutations in *Bifidobacterium*.

2.6 Future Perspectives

In recent years, CRISPR-Cas9 has enabled targeted gene editing in variant species [68]. CRISPR (Clustered Regularly Interspaced Short Palindromic Repeats) are short sequences identified in bacterial genomes as results of viral DNA invasion. Transcription of the CRISPR-array yields RNA fragments called CRISPR-RNA (crRNA). The crRNA directs the Cas9 nuclease to the target DNA (also called Spacer)

adjacent to a Protospacer-Adjacent Motif (PAM) (~4-5 base pairs downstream). The Cas9-mediated DNA cleavage results in a double-strand break (DSB) within the target DNA (~3-4 nucleotides upstream of the PAM sequence), intriguing DSB repair. During this process, mismatches or mutations on the target DNA are artificially introduced. The Cas9-induced DSB may be lethal to the bacteria [69]. However, assisted by DNA recombineering, CRISPR-Cas9 has been used as a counter-selection tool in generating mutants from *Lactobacillus reuteri* [70]. In this particular method, a single-stranded DNA (ssDNA) homologous to the target gene and a vector expressing the ssDNA-binding protein Beta, are introduced into the bacteria. Once Beta is expressed by the vector, it will combine the ssDNA and protect it from intracellular nuclease degradation. Due to the homology to the target gene, this ssDNA can be recognized by DNA polymerases as a template for DNA replication and incorporated into the synthesis of lagging strand. Mismatches or mutations are introduced at the target gene once the ssDNA is extended into a new daughter strand [71]. Mutants harboring the point-mutations from DNA recombineering will not be recognized by Cas9 and can survive during the selection. The wild-type cells with no DNA recombineering still have PAM sequence and will be cut by Cas9. The CRISPR-Cas9-assisted recombineering applied in *Lactobacillus* reduces the labor for selecting mutants and is a promising technique to apply to *Bifidobacterium*. However, the use of multiple shuttle vectors in this method might be a challenge for *Bifidobacterium*, as there have been no trials on transferring more than one shuttle vector into the bifidobacterial cells so far. Compared to *Lactobacillus*, *Bifidobacterium* are proposed to be more recalcitrant to genetic manipulations [72]. To our knowledge, there has been no report on using CRISPR-Cas9 to generate mutants from the genus of *Bifidobacterium*. The development of methodologies such as CRISPR-Cas9 to facilitate the genetic accessibility will be

promising and significant for functional genomic analyses of the genus of *Bifidobacterium*.

CHAPTER 3

THE CATALYTIC UREASE SUBUNIT UREC IS CRITICAL FOR *BIFIDOBACTERIUM LONGUM* UREA UTILIZATION

Yang Lyu¹, Korin Albert^{1,2}, Doyle Ward³, and David A. Sela^{1,2,3,4*}

¹Department of Food Science, University of Massachusetts, Amherst, MA 01003

²Molecular and Cellular Biology Graduate Program, University of Massachusetts,
Amherst, MA 01003

³Department of Microbiology and Physiological Systems, University of
Massachusetts Medical School, Worcester, MA 01655

⁴Department of Microbiology, University of Massachusetts, Amherst, MA 01003

3.1 Introduction

It has been widely reported that the infant microbiota plays a vital role during infant early development before weaning. Certain components from breast milk selectively enrich beneficial microbes in the infant microbiota and shape its configuration. Human milk oligosaccharides (HMOs), a category of soluble but non-digestible carbohydrates to the neonates, can enhance the growth of bifidobacteria [73-75]. While HMOs maintain the predominance of certain infant gut microbial cohorts, the bioavailability of consumed nitrogen sources in the lower infant gut is unclear. Compared to bovine milk, human milk contains less protein but more non-protein nitrogen (NPN) [12]. Interestingly, urea is one of the major forms and its proportion amounts to ~15% of the total nitrogen in human milk [76]. The discovery of urea metabolism genes in *Bifidobacterium longum* subsp. *infantis* ATCC15697 may be correlated with human milk nitrogen in the nursing infant gut microbiome [77]. The urea metabolism proteins include a transport system (*urtA*, *urtB*, *urtC*, *urtD*, *urtE*), *ureAB*, urease subunit gamma/beta, *ureC*, urease subunit alpha, and urease accessory proteins (*ureE*, *ureF*, *ureG*, *ureD*), which are highly specific to the subspecies of *B. infantis* [78]. Urease (EC 3.5.1.5), which degrades urea into ammonia and carbon dioxide, is widely distributed in bacteria including *Helicobacter pylori*, *Staphylococcus*, *Lactobacillus*, and *Proteus*. Specifically, in *H. pylori*, urease has been found to facilitate colonization of the stomach by elevating pH [79]. As for *B. infantis*, the function of this urease gene island is still under investigation. Although the identification of the urease gene island has been relatively recent, the production of urease by bifidobacteria was analyzed by Matteuzzi *et al.* in the species *B. suis* in 1973. They found 74% of the tested *B. suis* strains possess this enzyme [80]. In addition, Suzuki *et al.* studied the urease activity of bacteria isolated from human infant feces and found that all *B. infantis*

are urease positive [81]. Later on, Crociani *et al.* surveyed 414 bifidobacterial strains representing 21 species, and found that all *B. infantis* and some *B. breve* hydrolyzed urea, while *B. suis* was the strongest ureolytic species [82]. These early studies indicated that urease activity is dispersed in various species and subspecies of the genus *Bifidobacterium*. However, the driving force for retention of urease genes within *Bifidobacterium* genome is still poorly understood.

Given that *Bifidobacterium* correlates tightly with the infant host regarding human milk nutrients, it is natural to hypothesize a potential utilization of human milk urea by these microbes. In 1969, researchers tracking labelled ammonium-15N in child malnutrition indicated that labelled ammonium may be incorporated into blood cells and plasma protein, providing essential nitrogen in the malnourished state [83]. In 1992, Heine *et al.* used 15N-labeled *B. breve* to track whether bifidobacterial nitrogen can be absorbed by the infant. Results showed that 90% of 15N-labeled *B. breve* nitrogen was absorbed and 70% was retained in the infant protein pool, indicating a nutrient flow from the microbes to the host [84]. Fuller *et al.* brought forward the concept of urea nitrogen salvaging (UNS), a process of bacteria-induced colonic urea recycling in which enterocytes can actively transport urea into the intestinal lumen for bacterial usage [85]. Millard *et al.* used 15N-labeled urea to track ammonia hydrolyzed from infant bacteria and observed an increased supply of lysine and other indispensable amino acids to the infant host, supporting the hypothesized model of urea nitrogen salvaging by the infant gut microbiota [86].

The mechanism of bifidobacterial urease activity and its interactions with human milk urea remains elusive. To understand bifidobacterial urea utilization, molecular tools for genetic manipulation are necessary for investigating urease gene

activity in sufficient detail. While restriction-modification systems (R-M systems) are still one of the major barriers to gene modification [27], targeted mutagenesis has been successful in few strains [27, 28]. Here, we developed a urease deficient mutant from a urease-positive strain *Bifidobacterium longum* subsp. *suis* UMA399 via chemical mutagenesis. This mutant model has allowed us to initially investigate the genetic basis and functional characteristics of bifidobacterial urease in greater depth than previous studies.

3.2 Material and Methods

3.2.1 Bacterial Strains and Culture Conditions

Bacterial strains in this study are listed in Supplemental **Table A1**. Single colonies of bifidobacteria were grown overnight in De Man-Rogosa-Sharpe (MRS) broth (Difco, USA) supplemented with 0.05% (wt/v) L-cysteine and incubated overnight at 37°C in a Coy anaerobic chamber (Coy Laboratory Products, MI). *Escherichia coli* strains were grown in Luria-Bertani (LB) broth. For selecting *E. coli*, LB was supplemented with 20 mg mL⁻¹ chloramphenicol for pDOJHR, 34 mg mL⁻¹ for Rosetta (DE3) and 50 mg mL⁻¹ kanamycin for pSMT3, respectively. For bifidobacteria, the using of 5 µg mL⁻¹ chloramphenicol in MRS media was previously determined by a MIC (minimal inhibitory concentration) assay.

3.2.2 Mutant generation by Ethyl methane sulfonate (EMS)

Bifidobacterial cells from a 4 mL of overnight culture were spun down and resuspended in 4.75 mL phosphate buffer [pH7.2]. A 250 µL of EMS (99%) was added to reach a final concentration of 5% (v/v). The mixture was incubated at 37°C for 30 min. Cells were pelleted again and washed 3 times with fresh MRS. Cells suspension in 5 mL fresh MRS was diluted to 25% of the original concentration and grown

overnight. Dilutions of 100 μ L overnight mutagenized cultures were spread on a urease differential agar optimized from Monnet *et al.* [87]. The urease differential agar was made from GAM Broth (HI-Media, India) supplemented with 0.5% (wt/v) glucose, 0.001% bromothymol blue, and 4.5% (wt/v) urea. Plates were incubated anaerobically at 37°C for 5 days. Whitish colonies (as opposed to the urease-positive dark green colonies) were selected and cultured for genomic DNA extraction and sequencing.

3.2.3 Genome Sequencing and SNP Analysis

Genomic DNA was extracted from 5 mL overnight cultures using the MasterPure Gram-positive DNA purification kit (Epicentre [an Illumina Company], Madison, WI). DNA quality and quantity were determined using a NanoDrop 2000 Spectrophotometer and a Qubit 2.0 Fluorometer (ThermoFisher, USA), respectively. Sequencing libraries were prepared using the Nextera XT 150-bp paired-end library preparation kit (Illumina, San Diego, CA). Whole-genome sequencing was performed on the Illumina NextSeq platform using v2 reagents. Reads were assembled *de novo* via SPAdes version 3.9.1 and the assemblies were improved using Pilon version 1.22 (Bankevich, 2012; Walker, 2014). Both analyses were conducted using the Massachusetts Green HighPerformance Computing Center (mghpcc.org). Gene model predictions and annotations were performed using the Rapid Annotation using Subsystem Technology (RAST) annotation service (Overbeek, 2013). Single nucleotide polymorphisms (SNP) were detected in the annotated wild-type and mutant genome using the PATRIC version 3.5.30 Variation Analysis Service (Wattam, 2016) via the aligner (BWA-mem-strict) and the SNP caller (FreeBayes). The urease gene cluster of *B. suis* UMA399 and *B. infantis* UMA272 was depicted by SimpleSynteny version 1.4 [88].

3.2.4 Microplate Growth Assay

The growth phenotype of cells was monitored in a 96-well plate. Cells from overnight MRS broth culture were used to inoculated at 1% (v/v) complex nitrogen and urea broth modified from a basal medium (v/v) (2% lactose, 0.2% potassium phosphate dibasic anhydrous, 0.3% sodium acetate anhydrous, 0.02% magnesium sulfate heptahydrate, 0.0038% manganese (II) sulfate monohydrate, 0.1% Tween 80, and 0.022% L-cysteine). For the complex nitrogen media, an extra 1% peptone, 0.8% yeast extract, and 0.1% ammonia citrate were added to the basal medium. For the urea broth, an extra 2% urea was added to the basal medium as a primary nitrogen source. Growth in basal media was regarded as the negative control. The growth assay was conducted at 37°C for 4 days in a microplate spectrophotometer (BioTek, USA) placed within the anaerobic chamber. Reads were performed with shaking at intervals of 5 min to detect optical density at 600 nm. Each strain was measured in biological triplicate with three technical repeats.

3.2.5 Determination of Urease Activity

The urea assay was optimized for bifidobacteria based on a modified phenol-hypochlorite assay [89]. Cells were harvested from 2 - 5 mL overnight culture and washed three times with pre-chilled 25 mM HEPES buffer [pH 7.0]. A 2 mL volume of cell resuspension in 25 mM HEPES was transferred to the lysing matrix E tube (MP Biomedicals, USA) and was subjected to a FastPrep-24TM 5G homogenizer (MP Biomedicals, USA). The bead-beating was done at a speed of 3.5 m/s for 30 s, three times, with a chilling period between each round. Tubes were centrifuged at 16,200 × g for 10 min and the supernatant was kept. The cell protein concentration was measured by Pierce BCA protein Assay kit (ThermoFisher, USA) on a NanoDrop (ThermoFisher, USA). For the urease assay, 20 µL of proper diluted lysates were incubated with 20 µL of urea buffer (25 mM HEPES [pH 7.0] plus 300 mM urea) in 96-well plates at 37°C

for 30 min. Then 75 μ L of phenol plus nitroprusside was added to terminate the reactions, followed by an equal volume (75 μ L) of alkaline hypochlorite. The mixture was incubated at 37°C for 30 min. The absorbance at 620 nm was measured using a plate reader (SpectraMax i3x, Molecular Devices, USA). The amount of ammonia generated was calculated from a standard curve (0 - 50 nmol) made with ammonium chloride dissolved in 25 mM HEPES [pH 7.0]. Urease activity was defined as nanomoles of ammonia produced per minute per milligram of protein [$\text{nmol NH}_3 \text{ min}^{-1} (\text{mg protein}^{-1})$]. To avoid the influence of ammonia released from urease-independent reactions, cell free lysates in each replicate were incubated with 25 mM HEPES [pH 7.0] and the values of ammonia produced from these reactions were subtracted. Urease activity of each strain was calculated as means of biological triplicates with three technical repeats.

3.2.6 The Construction of the UreC expression Vector

The expression vector pSMT3 was a generous gift from Prof. Stratton from the University of Massachusetts Amherst. Genomic DNA from bifidobacteria was extracted using the MasterPure Gram positive DNA purification kit (Epicentre Biotechnologies). The *ureC* coding sequence (CDS) was amplified by primer PSM-F/R with Q5 High-fidelity DNA polymerase, in which *Bam*HI and *Xho*I sites were inserted. The PCR products were purified using a QIAquick PCR purification kit (Qiagen). Purified Amplicon and pSMTS were digested with *Bam*HI and *Xho*I, then cleaned by Zymoclean Gel DNA Recovery Kit (Zymo Research). Ligation was done with T4 DNA ligase (NEB) at 16°C overnight then chemically transferred into *E. coli* NEB 5-alpha (NEB, USA). All reagents were used according to the manufacturer's instructions. The transformants were confirmed further by linearization with *Bam*HI and *Xho*I before being subjected to insert sequencing by Genewiz (Boston, USA). The pSMT3 vector

with wild-type or mutant *ureC* was named pSMT-U, as shown in **Figure A4** drawn by SnapGene (from GSL Biotech; available at snapgene.com).

3.2.7 Purification of UreC and In Vitro Urease Activity

The vector pSMT-U was chemically transformed into *E. coli* Rosetta (DE3) for protein overexpression. Single colonies were grown in 5 mL cultures (LB kana/cam) overnight at 37°C. Then, 1% (v/v) of this overnight culture was inoculated into 70 mL LB (kana/cam) and grown until OD_{600 nm} reached 0.8 - 1.0. Isopropyl β-D-thiogalactoside (IPTG) was added to the culture to a final concentration of 0.1 mM. The mixture was incubated at 32°C for 4 hours with shaking (250 rpm). Cells were harvested by centrifugation and sonicated in 8 mL phosphate buffer (pH 7.4) via a Microson Ultrasonic Cell Disruptor (Microson, USA) using six 10-second bursts at high intensity with a 10-second cooling between each burst for 30 min. Cell suspensions were centrifuged at 4,696 × *g* for 5 min to remove the cellular debris. Then, 8 mL of the supernatant was purified using the HisPur Ni-NTA Spin Columns (ThermoFisher, USA), washed with 25mM imidazole (phosphate buffer [pH 7.2]) twice, 60 mM imidazole (phosphate buffer [pH 7.2]) once, and then was eluted three times by 250 mM imidazole (phosphate buffer [pH 7.2]) as the 6xHis-SUMO-UreC. Imidazole in the protein suspension was removed by desalting through the Amicon Ultra-15 Centrifugal Filter Unit (30kDa MWCO) (Millipore, USA) against the buffer (50 mM Tris-HCl, 150 mM NaCl, pH 8.0) at 4°C. L at 4°C overnight. To cleave the 6xHis-SUMO tag, the protein mixture after desalting was incubated with SUMO protease in buffer (50 mM Tris-HCl, 150 mM NaCl, pH 8.0) supplemented with 1mM DTT at 4°C overnight. After cleavage, DTT in the protein was removed by desalting against 10 mM imidazole in PBS buffer (20 mM sodium phosphate, 300 mM NaCl, pH 7.4) in Amicon Ultra-15 Centrifugal Filter Unit (30kDa MWCO) and run through the NI-NTA column again to

remove the 6xHis-SUMO tag. Purified UreC in the flow through was kept at 4°C shortly and immediately used for *in vitro* urease activity measurements. The *in vitro* urease activity assay was based on a previous study [90]. Mutant cell free lysates were prepared by bead-beating. The bead-beating was done at a speed of 3.5 m/s for 30 s, three times, with a chilling period between each round. Tubes were centrifuged at $16,200 \times g$ for 10 min and the supernatant was kept. The cell protein concentration was measured by Pierce BCA protein Assay kit (ThermoFisher, USA) on a NanoDrop (ThermoFisher, USA). A 12 μL (~20 μg) purified wild-type UreC or Mut UreC was incubated with 12 μL mutant cell free lysates in 12 μL of 25 mM HEPES buffer. The solution was incubated at 25°C for 24 hours and then at 37°C for 12 hours. To determine the urease activity, 5 μL of the incubated solution was added to 245 μL of reaction buffer (50 mM HEPES, 25 mM urea [pH 7.0]) and incubated for 30 min. Then, 375 μL of phenol plus nitroprusside was added to terminate the reactions. An equal volume (375 μL) of alkaline hypochlorite was then added and incubated at 37°C for 30 min. The amount of ammonia generated was calculated from a standard curve (0 - 5 nmol) made with ammonium chloride dissolved in 25 mM HEPES [pH 7.0]. Urease activity was defined as nanomoles of ammonia produced per minute per milligram of protein [$\text{nmol NH}_3 \text{ min}^{-1} (\text{mg protein}^{-1})$].

3.2.8 Differential Scanning fluorimetry (DSF)

To compare the difference of nickel binding between the mutant and wild-type UreC. A differential scanning fluorimetry of both proteins incubated in Ni^{2+} was performed according to Niesen *et al.* [91]. Specifically, nickel chloride was dissolved in 100% DMSO with a final concentration of 400 μM . Then, the 100% DMSO was diluted into 10 mM HEPES [pH 7.0] in a ratio of 1:1000. A 4.2 mL purified UreC in 10 mM HEPES [pH 7.0] solution was mixed with 5 x SYPRO Orange fluorescence dye

(ThermoFisher, USA). Samples were added to a 96-well plate. In each well, 39 μL of protein solution and 1 μL of Ni^{2+} were mixed, with a final Ni^{2+} concentration of 10 μM . The plate was then covered with a foil seal (Agilent Technologies), centrifuged to avoid bubbles, and measured on 7500 Fast Real-Time PCR System according to the settings outlined in Niesen *et al.* Each group was measured in 6 technical replicates.

3.2.9 Construction of the UreC expression Shuttle Vector

DNA manipulations and molecular techniques were conducted as described above. The *E. coli-Bifidobacterium* shuttle vector pDOJHR was a kind gift from Prof. Sullivan [26]. The ~ 100 bp upstream and ~ 60 bp downstream regions flanking the *ureC* coding sequence (CDS) were amplified by primer PD-F/R, in which *EcoRI* sites were incorporated. For the construction of pDOJ-U, the amplicon and pDOJHR were digested with *EcoRI*, ligated by T4 DNA ligase, and transferred to *E. coli* strain NEB 5-alpha (NEB, USA). The insert within the plasmid was sequenced by Eton Bioscience (Boston, USA) to ensure that only the right DNA fragments had been introduced.

3.2.10 Electroporation and Plasmid Isolation from the Mutant

A 5% (v/v) overnight culture of the mutant strain was used to inoculate 40 mL MRS (Difco, USA) supplemented with 0.05% L-cysteine and incubated at 37°C until an $\text{OD}_{600\text{ nm}}$ of 0.4-0.5 was reached. Cells were collected at $4,696 \times g$ for 15 min at 4°C, then washed 3 times with 30 mL ice-cold electroporation buffer [10% (v/v) glycerol and 0.5 M sucrose]. Cells were resuspended in 1 mL buffer in a microcentrifuge tube, pelleted again, and resuspended in 1/250 (v/v) of the original culture. For each transformation, 50 μL of the cell suspension and 400 ng of plasmid DNA were mixed and incubated on ice for 30 min, then transferred to a pre-chilled 1 mm disposable cuvette. A voltage electric pulse was delivered through a Gene Pulser (Bio-Rad) at 25 μF , 200 Ω and 2.2 kV. Cells were immediately resuspended with 950 μL of MRS

(Difco, USA), transferred into a 15 mL falcon tube, and recovered anaerobically for 3 hours at 37°C. After which, cells were diluted and plated on aluminum foil-wrapped MRS plates supplemented with 5 µg mL⁻¹ chloramphenicol and incubated anaerobically at 37°C for 48 -72 h. Transformation efficiency was calculated as number of transformants obtained per µg of plasmid DNA [colony-forming unit (CFU) per µg DNA]. Plasmid isolation from bifidobacteria transformants was optimized from Francesca *et al.* [92]. A 10 mL overnight culture of mutant transformed with pDOJHR or pDOJ-U was used. Plasmid prep was performed using the QIAprep Spin Miniprep kit (Qiagen) with an additional step for cell lysis. Cells were suspended in Buffer P1 with a final concentration of 30 mg mL⁻¹ lysozyme and incubated for 1hour at 37°C. Extracted plasmids were chemically transformed back into E. coli to propagate and were linearized for identification.

3.2.11 Statistical Analysis

All analyses were performed with GraphPad Software Prism 8.0.1 (GraphPad Software, Inc., CA, USA). Results were shown as mean ± standard deviation (*SD*). The models were checked for normality and variance homogeneity and data transformation was performed when necessary. Urease activity of multiple strains grown in complex nitrogen was analyzed through one-way analysis of variance (ANOVA) followed. Urease activity or growth phenotype of multiple strains cultured from variant media, including 2% urea, 2% urea plus Ni²⁺, complex nitrogen, and the negative control was compared by two-way ANOVA with Tukey's multiple comparison test. Urease compliment by purified UreC was analyzed by unpaired two-tailed t-test (WT UreC vs. boiled WT UreC; Mut UreC vs. boiled Mut UreC) and unpaired two-tailed t-test (WT UreC vs. Mut UreC), respectively. *P* < 0.05 was classified as significant.

3.2.12 Protein Structure Stability Prediction

The structural stability of the mutant UreC was predicted at STRUM (<https://zhanglab.ccmb.med.umich.edu/STRUM/>) using Mode I: Single-point mutations [93]. The 3D structure of UMA399 UreC was predicted by SWISS-MODEL (<http://swissmodel.expasy.org/>) [94] and visualized by Chimera 1.13.1 (<http://www.rbvi.ucsf.edu/chimera>) [95].

3.2.13 Phylogenetic Analysis

The bifidobacterial *ureC* protein sequences were retrieved from Integrated Microbial Genomes (IMG) in DOE Joint Genome Institute (JGI; <http://img.jgi.doe.gov>). The multiple sequence alignment was done by MAFFT program with default settings [96]. For the phylogenetic analysis of *ureC*, the alignments were exported in PHYLIP format and was imported into PhyML 3.0 [97] where a maximum likelihood phylogenetic tree was constructed by the SMS (Smart Model Selection) [98] using the default settings. The phylogenetic tree was visualized using FigTree [99]. Distribution of urease genes in *Bifidobacterium* was generated by pheatmap RStudio Team (2018). RStudio: Integrated Development for R. RStudio, Inc., Boston, MA URL <http://www.rstudio.com/>. Each gene count was retrieved from the PATRIC- version 3.5.30 Comparative Pathway Service (Wattam, 2016).

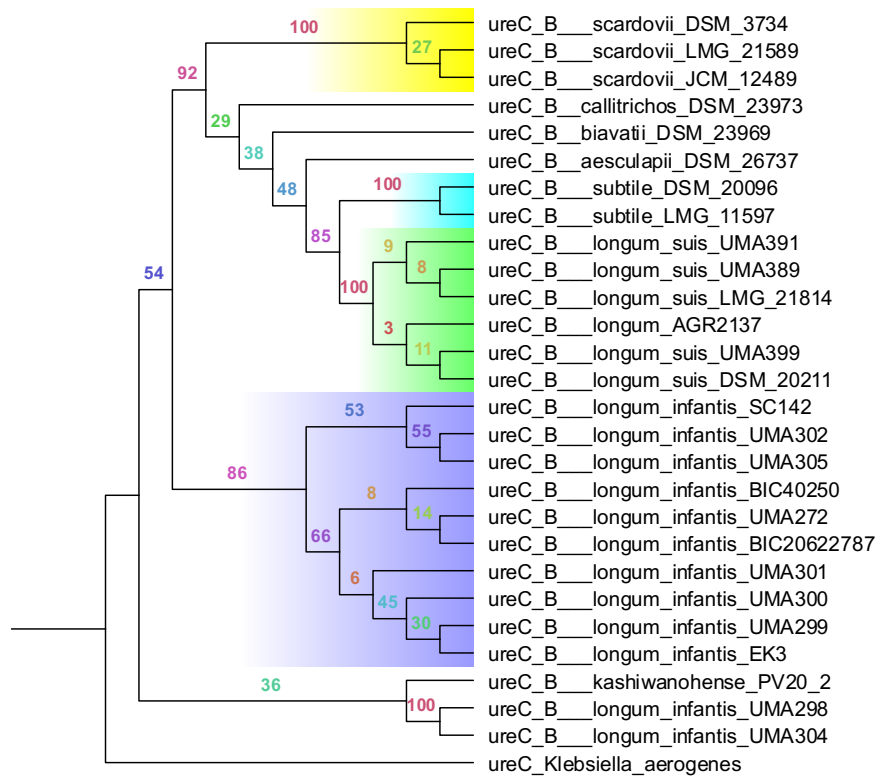
3.3 Results

3.3.1 Urease activity is strain-dependent and is elevated by urea and Ni²⁺.

To detect bifidobacterial ability of hydrolyzing urea, four strains carrying the urease gene cluster from the subspecies of *B. infantis*, and *B. suis* were tested for their ability to hydrolysis urea and produce ammonia after grown from MRS culture. *B. longum* UMA306, which does not possess urease genes, was negative control. UMA399 shows the highest activity, 10 to 60-fold higher than *B. infantis* strains.

Among all *B. infantis*, UMA302 exhibits higher activity than UMA272 and UMA299. The latter two strains had no difference in activity ($P = 0.2516$), as shown in **Figure 3**. Phylogeny analysis of the *ureC* genes in *Bifidobacterium* suggested a (sub) species-variance (**Figure 2**).

As we found from other bacterial species, the concentration of urea (as the substrate) and nickel (as the cofactor) may influence the urease activity. To test if the concentration of urea and nickel will impact bifidobacterial urease, we measured the urease activity of *B. infantis* strains grown in complex nitrogen, 2% urea, and 2% urea with 50 μM Ni^{2+} (**Figure 4**). Results showed that the urease activity of all *B. infantis* strains in 2% urea is greatly elevated, 4 to 10-fold higher than the urease activity in complex nitrogen. The addition of 50 μM of Ni^{2+} to the 2% urea media resulted in higher urease activity than 2% urea media alone. Previously, UMA302 showed significantly higher urease activity than UMA272 ($P = 0.0014$) and UMA299 ($P = 0.0016$) in complex nitrogen (**Figure 3**). However, this difference could not be identified from bacterial cells grown in 2% urea and 2% urea with 50 μM Ni^{2+} ,



2.0

Figure 2 Maximum likelihood phylogenetic analysis of the bifidobacterial UreC protein.

Bootstrap values are shown on each node. Number of bootstrap replicates is 100.

Different colors highlight the clustered (sub) species.

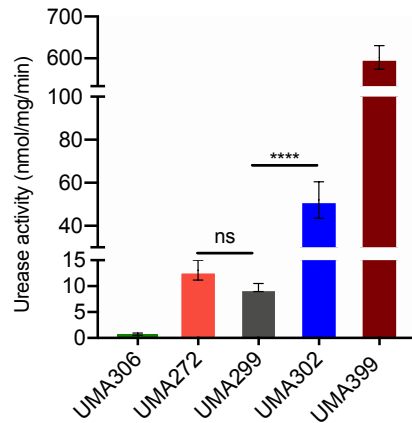


Figure 3 Urease activity among multiple bifidobacterial strains cultured from complex nitrogen.

UMA272, UMA299, and UMA302 are *B. infantis* strains; UMA399 is a *B. suis* strain; UMA306 is a *B. longum* strain demonstrated with no urease activity previously (data not shown) and is used as negative control. Urease activity was detected by the generation of ammonium in nanomole per milligram protein per min [$\text{nmol NH}_3 \text{ min}^{-1} (\text{mg protein}^{-1})$]. The bars represent the mean \pm *SD* (standard deviation) of three individual biological replicates ($n = 3$). Significant differences between strains were evaluated by one-way ANOVA and Tukey's multiple comparison test; NS (not significant; $P > 0.05$), **** $P < 0.0001$.

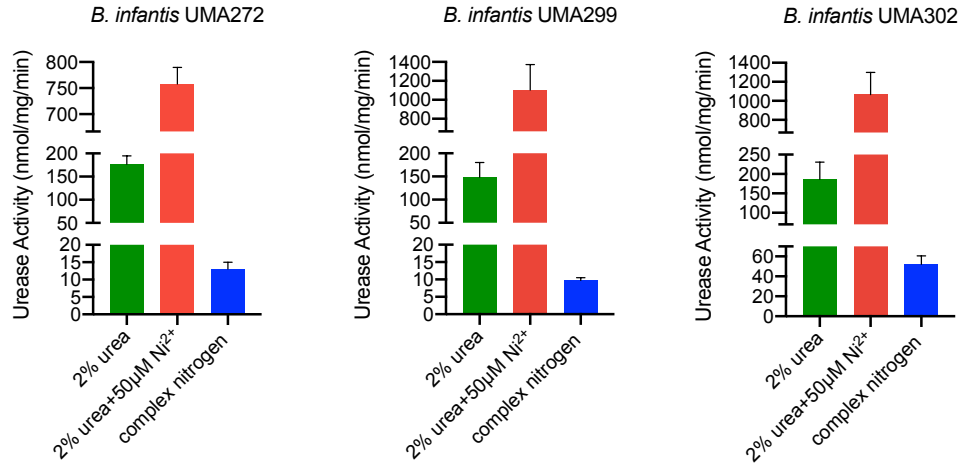


Figure 4 Urease activity among multiple bifidobacterial strains cultured from complex nitrogen.

The bars represent the mean \pm *SD* (standard deviation) of three individual biological replicates ($n = 3$). Significant differences between the strains were evaluated by two-way ANOVA and Tukey's multiple comparison test; $P < 0.05$ was classified as significant.

3.3.2 A urease-deficient mutant from *B. suis* UMA399 was selected and identified

The UMA399 colonies appeared dark green on urease differential agar after incubation. This is the result of ammonia production. We hypothesized that the urease mutant would not utilize urea normally and may not produce ammonia, resulting in a lighter color than the wild-type dark green phenotype. Following this hypothesis, we performed several trials of chemical mutagenesis to identify mutants by their phenotype on urease differential agar. The colony exhibits a whitish color was posited to have a urease mutation and selected for further analysis. As shown in **Figure 5A**, the mutant has no urease activity compared to the negative control ($P = 0.8137$), while the wild-type showed consistent strong activity. The mutant's growth phenotype is depicted in **Figure 5B**, which shows that the mutant did not grow (maximum $OD_{600\text{ nm}} = 0.103 \pm 0.005$) in 2% urea media compared to the negative control (maximum $OD_{600\text{ nm}} = 0.08$

± 0.006 ; $P = 0.8137$), in contrast to the wild-type (maximum $OD_{600\text{ nm}} = 0.273 \pm 0.049$; $P < 0.0001$). These observations indicated that the whitish colony was confirmed as a urease-deficient mutant.

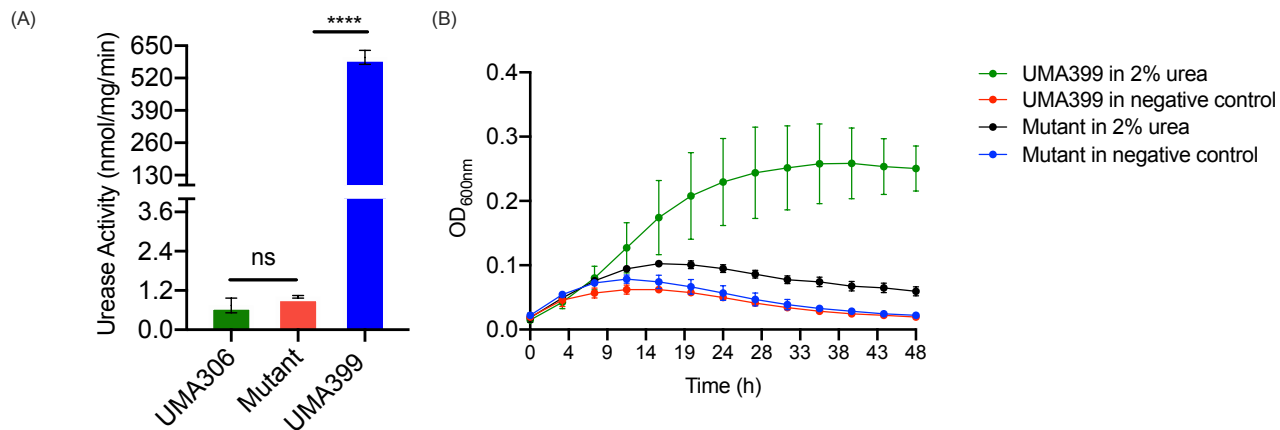


Figure 5 Urease activity (A) and growth ability of the mutant strain in 2% urea as a primary nitrogen source (B).

The *B. suis* UMA399 mutant strain was selected following EMS mutagenesis. Strains were all cultured from complex nitrogen. UMA399 is the wild-type strain; UMA306 is the urease negative strain. In panel (A), the bars represent the mean \pm SD (standard deviation) of three individual biological replicates (n = 3). Significant difference was evaluated by one-way ANOVA and Tukey's multiple comparison test; NS (not significant; $P > 0.05$), **** $P < 0.0001$. In panel (B), X axis indicates the time points in 48 hours; Y axis shows the optical density at 600 nm. Growth curves includes, Green: UMA399 in 2% urea; Red: UMA399 in negative control; Black: mutant in 2% urea; Blue: UMA399 in negative control. UMA399 is the wild-type strain. The continuous growth curves display the optical density at 600 nm at each time point by mean \pm SD (standard deviation) from three individual biological replicates (n = 3).

3.3.3 EMS mutagenesis resulted in a nonsynonymous mutation on the mutant *ureC* gene

To identify any potential urease gene mutation, the wild-type and the mutant

genomes were sequenced. SNP-Calling identified 89 nonsynonymous mutations, 36 synonymous mutations, and one deletion on the mutant chromosome. All mutations were caused by C/G-to-A/T transversions, which corresponded to the known effects of EMS mutagenesis [100]. As shown in **Figure 6A**, the urease gene cluster of UMA272 and UMA399 all consist of a urea ABC transporter (*urtB/C/D/E* plus a urea binding protein), a nickel ECF transporter (*nikM/N/O/Q*), urease alpha and gamma subunits (*ureC/ureAB*), and accessory proteins (*ureE/F/G/D*). The distribution of urease genes in some bifidobacterial strains is shown in **Figure 6B**). Strains from *B. infantis*, *B. suis*, *B. callitrichos*, *B. kashiwanohense*, *B. scardovii*, *B. biavati*, and *B. subtile* harbors a complete urease gene cluster. It is interesting that all the three *B. bifidum* strains only contains a *urtE* gene, while the rest of urease genes are missing. Also, even though most urease genes are found in *B. infantis*, *B. infantis* 157F-NC does not show existence of the gene cluster. Throughout the mutant urease gene cluster, only one nonsynonymous mutation was found in the *ureC*, encoding the urease alpha subunit. The mutation caused the conversion of glutamic acid residue to a lysine residue in the protein sequence. To check if this single-mutation affects the protein stability, the mutant protein sequence was analyzed by STRUM (structure-based prediction of protein stability changes upon single-point mutation) (**Table 1**). The free energy gap difference ($\Delta\Delta G$) between the wild-type UreC and the mutant UreC was -1.56, suggesting that the single-point mutation may cause structural destabilization in the mutant UreC.

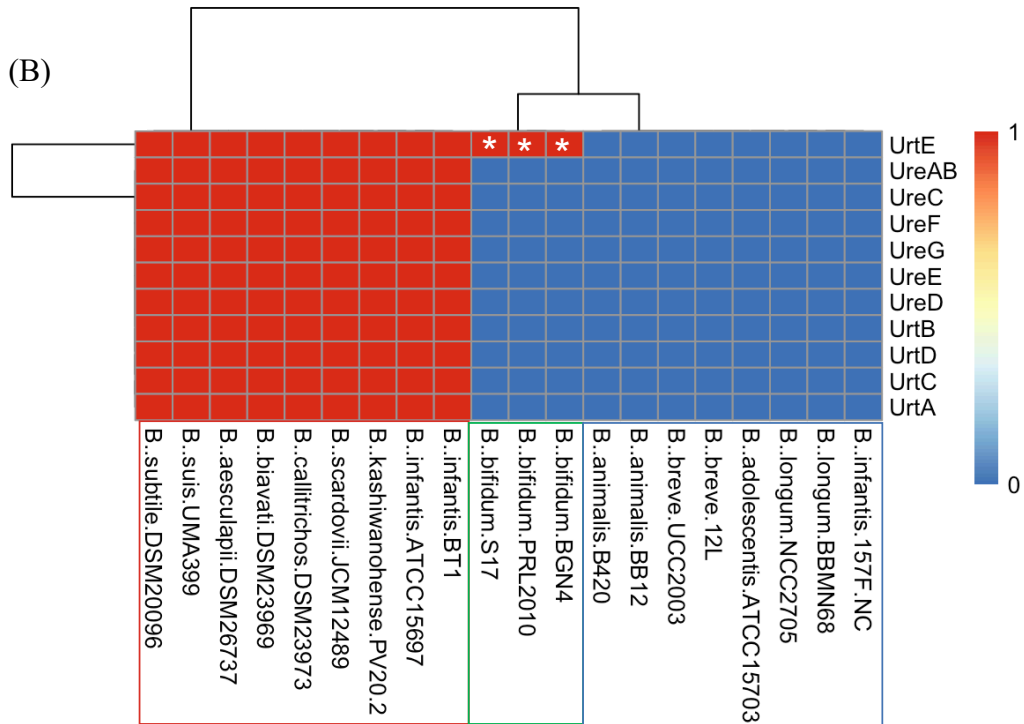
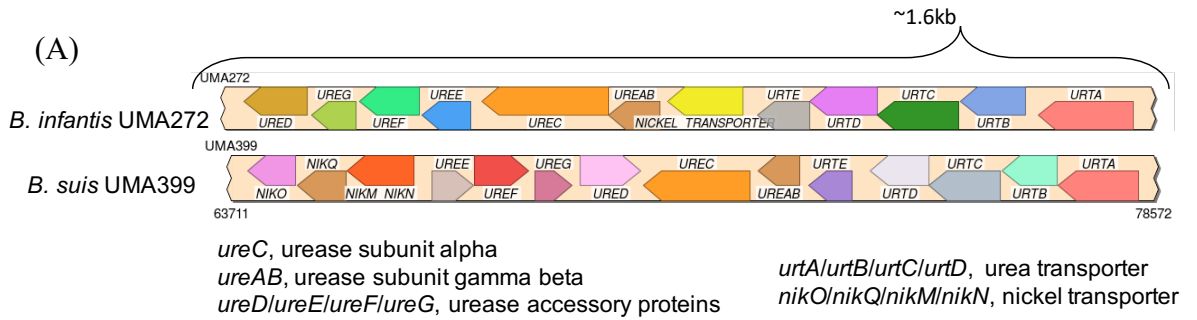


Figure 6 Urease gene cluster of *B. suis* UMA399 and *B. infantis* UMA272 (A) and Distribution of urease genes on variant bifidobacterial genomes (B).

In panel (A), colored arrows denote all the genes on the cluster. In panel (B), X (horizontal) axis indicates bifidobacterial strains. Y (vertical) axis shows the number of each urease gene from the cluster, from up to down: *urtE*, *ureAB*, *ureC*, *ureF*, *ureG*, *ureE*, *ureD*, *urtB*, *urtD*, *urtC*, *urtA*. The legend scale on the right indicate the gene counts found on the genome. Red: 1; Navy: 0. The white stars indicated the three *B. bifidum* strains each has one *urtE* gene. Groups of bifidobacteria with a complete urease gene cluster, a truncated urease gene cluster or without the gene cluster were marked in red, green and blue frame at the bottom.

Table 1 Prediction of wild-type UreC stability changes upon the single-point mutation by STRUM.

The mutation on the UreC caused the Glutamic acid (E) 343 to Lysine (K). The $\Delta\Delta G$ OR $\Delta\Delta G$ are the changes of Gibbs free-energy gap between the wild-type UreC and the mutant UreC. A value of $\Delta\Delta G$ under zero suggested that the single-point mutation caused a destabilization.

Position	Wild-Type	Mutant type	$\Delta\Delta G$
343	E	K	-1.56

3.3.4 Purified wild-type UreC restored urease activity after incubation with mutant lysates

To test if *ureC* mutation would cause protein-level functional deficiency, we expressed and purified both the wild-type UreC and the mutant UreC *in vitro*. The purified UreC were tested in a urease assay *in vitro*. Cell free lysate from the mutant strain was incubated with both purified UreC. After incubation, the wild-type UreC was able to restore urease activity to a lower level (**Figure 7**). The mutant UreC showed no difference from the negative control ($P = 0.061$), indicated its deficiency. This result suggested that the UreC was necessary for bifidobacterial urease function.

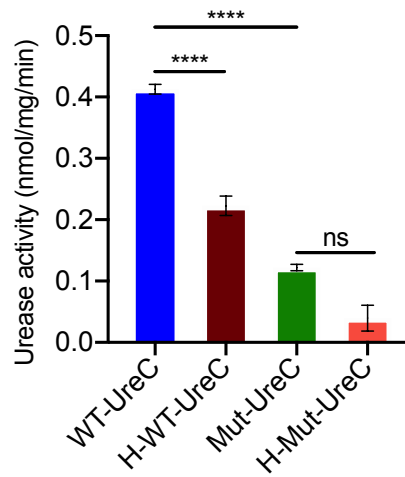


Figure 7 Urease activity was restored by purified UreC.

Mut-UreC: purified UreC from the mutant; WT-UreC: purified UreC from wild-type; H-WT/Mut-UreC means heated UreC, which is used as negative control. Purified UreC was incubated with the mutant cell-free lysates *in vitro*, supplemented with urea. The bars represent the mean \pm *SD* (standard deviation) of three independent experiments ($n = 3$). Significant differences were evaluated by t-test; NS (not significant; $P > 0.05$), **** $P < 0.0001$.

3.3.5 Purified mutant UreC is different in confirmation vs. WT UreC

The predicted protein structure of wild-type UreC from UMA399 is shown in **Figure A3**. Two green nickel ions were niched inside the red histidine, lysine and aspartate residues nearby. This tertiary structure predicts the metalcentre of the UreC as a monomer. Based this prediction, Ni^{2+} is the cofactor of UreC. UreC (alpha subunit) might bind to Ni^{2+} for urease maturation and will thus cause a conformation change during binding to nickel. The curve indicates SYPRO orange fluorescence intensity versus temperature. During UreC binding to Ni^{2+} , the protein would unfold and expose its hydrophobic patches, leading to a strong emission of fluorescent light of 610nm, and thus indirectly indicating configuration difference. The curved showed an excited peak from 50,000 to 80,000 (A.U.) at 610 nm when the wild-type UreC was incubated with

Ni²⁺. While the incubation of mutant UreC with Ni²⁺ showed no emission peak.

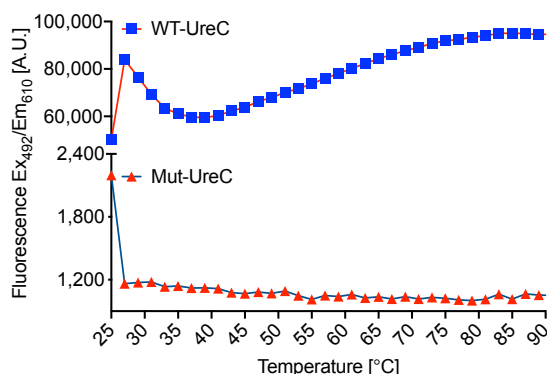


Figure 8 Configuration change of the wild-type UreC and mutant UreC detected by differential scanning fluorimetry.

The curve shows the SYPRO orange fluorescence intensity versus temperature during the incubation of purified UreC with Ni²⁺. While the protein subunit folded, the fluorescence intensity is excited by light of 492 nm. The unfolding of the protein or the large emission of the 610 nm by the fluorescence indirectly suggested a configuration change.

3.3.6 Transformation of pDOJ-U into the mutant complement urease activity

To restore urease activity *in vivo*, we cloned *ureC* with its promoter from the wild-type strain *B. suis* UMA399 into the shuttle vector pDOJHR. As shown in **Table 2**, the transformation of pDOJHR and pDOJ-U to the mutant gave an efficiency of $(1.375 \pm 0.71) \times 10^2$ and $(1.25 \pm 0.54) \times 10^2$ (CFU μg^{-1} DNA), respectively. Urease assay and growth in 2% urea were tested on mutants harboring the pDOJHR and pDOJ-U vectors (**Figure 10 and Figure 11**). The mutant with pDOJ-U vector showed the same level of urease activity (219.041 ± 69.081) [nmol NH₃ min⁻¹ (mg protein)⁻¹] to the wild-type (237.055 ± 59.463) [nmol NH₃ min⁻¹ (mg protein)⁻¹] ($P = 0.9838$). The mutant with the pDOJHR vector did not exhibit an activity compared to the negative control (**Figure 10**). Growth curve in **Figure 11** depicts a positive utilization of 2%

urea by the mutant containing pDOJ-U, with a maximum $OD_{600\text{ nm}} = 0.209 \pm 0.0147$, significantly higher than its negative control ($OD_{600\text{ nm}} = 0.079 \pm 0.004$; $P < 0.0001$) and same as the wild-type ($OD_{600\text{ nm}} = 0.273 \pm 0.495$; $P = 0.5877$). The mutant containing pDOJHR in 2% urea reached a maximum $OD_{600\text{ nm}} = 0.085 \pm 0.01327$, with no difference to its negative control ($OD_{600\text{ nm}} = 0.068 \pm 0.008$; $P = 0.9993$). Growth levels of all strains in complex nitrogen were similar, indicating that the shuttle vectors did not induce any toxic side effects. The results of these experiments demonstrate the ability to restore urease activity *in vivo* by expressing *ureC* only, indicating that the loss of urease function in the mutant was likely due to this mutation.

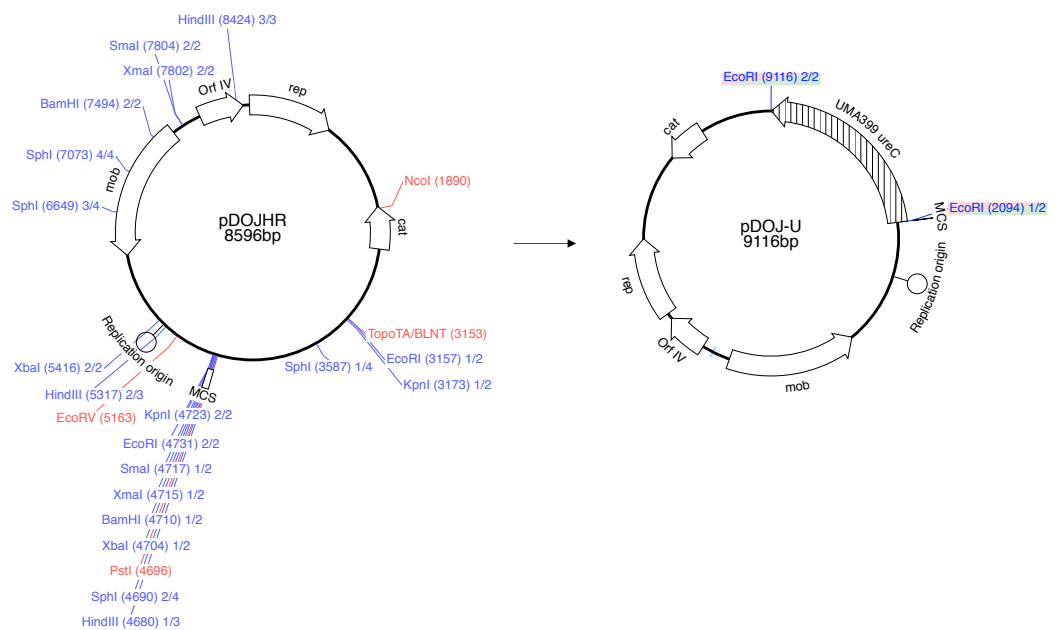


Figure 9 Construction of the UreC expression shuttle vector pDOJ-U.

The *ureC* fragment indicated by pattern-filled arrow was cloned in between the *EcoRI* sites on the shuttle vector pDOJHR, forming pDOJ-U.

Table 2 Electro-transformation efficiency.

pDOJHR and pDOJ-U were both transferred into the *B. suis* UMA399 mutant strain. Results were represented by mean \pm SD (standard deviation) from three independent experiments (n = 3). Transformation efficiency was calculated as number of

transformants obtained per μg of plasmid DNA in unit colony-forming unit (CFU) per μg DNA.

Host	Plasmid	Transformation efficiency (CFU μg^{-1} DNA)
Mutant	pDOJHR	$(1.375 \pm 0.71) \times 10^2$
Mutant	pDOJ-U	$(1.25 \pm 0.54) \times 10^2$

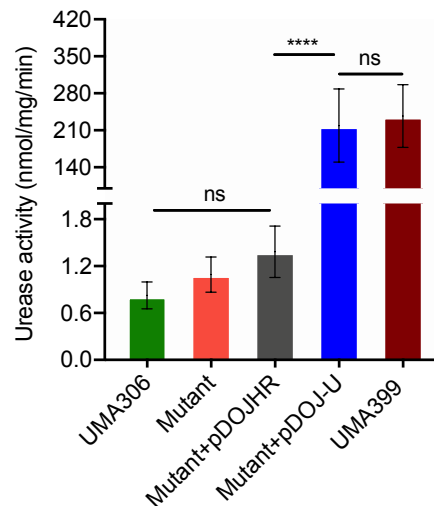


Figure 10 Urease activity was complemented by expressing the wild-type *ureC* gene in the mutant.

Strains were cultured in complex nitrogen. Mutant + pDOJHR: mutant transferred with pDOJHR; Mutant + pDOJ-U: mutant transferred with pDOJ-U (*ureC* from wild-type cloned in pDOJHR). UMA399 is the wild-type strain; UMA306 is the urease negative strain. The bars represent the mean \pm *SD* (standard deviation) of three individual biological replicates ($n = 3$), with the exception of pDOJ-U and UMA399 ($n=4$). Significant differences were evaluated by one-way ANOVA and Tukey's multiple comparison test; NS (not significant; $P > 0.05$), **** $P < 0.0001$.

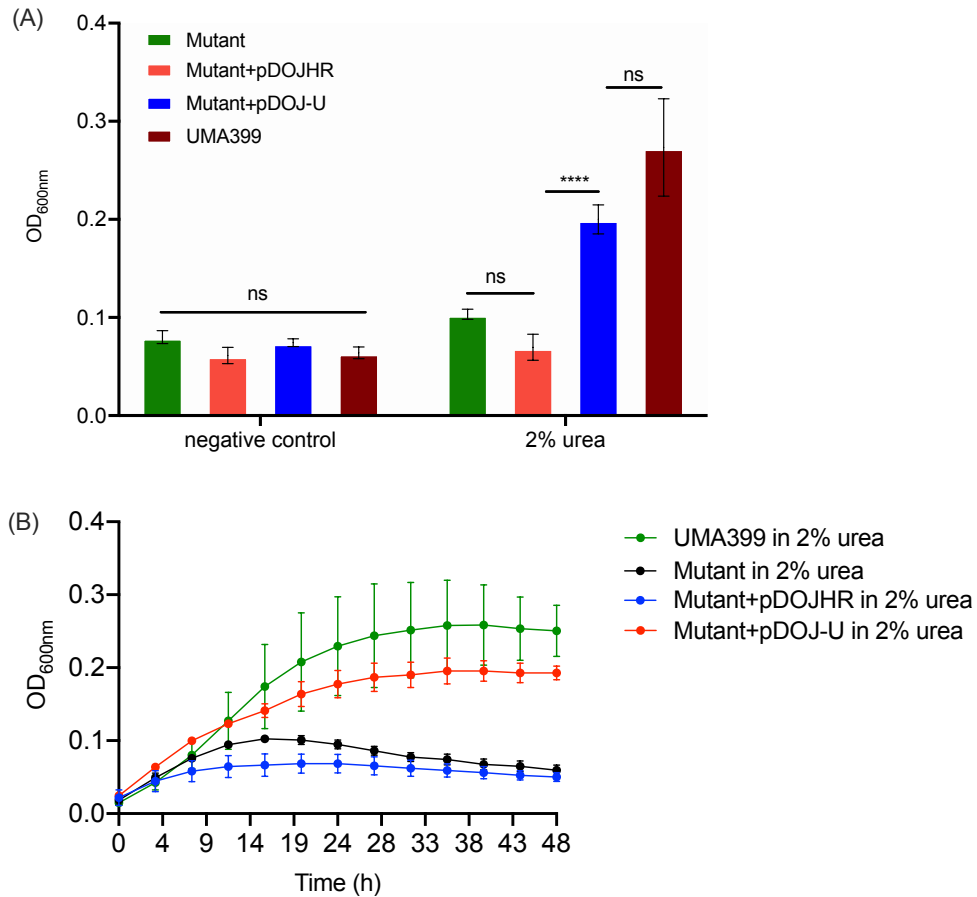


Figure 11 Growth phenotype complemented by pDOJ-U.

Strains were cultured in 2% urea and negative control. Mutant + pDOJHR: mutant transferred with pDOJHR; Mutant + pDOJ-U: mutant transferred with pDOJ-U (*ureC* from wild-type cloned in pDOJHR). UMA399 is the wild-type strain. In panel (A), the bars represent the maximum optical density at 600 nm of each strain in mean \pm *SD* (standard deviation) of three individual biological replicates ($n = 3$). Growth was compared by two-way ANOVA and Tukey's multiple comparison test; NS (not significant; $P > 0.05$), **** $P < 0.0001$. Panel (B) shows the entire growth pattern. The continuous growth curves display the optical density at 600 nm at each time point by mean \pm *SD* (standard deviation) from three individual biological replicates ($n = 3$).

3.4 Discussion

The significant proportion (~15%) of urea as a nitrogen source in human milk provides a secondary nutrient reservoir if the infant microbiota utilizes it and make it

absorbable by the infant, as 95% of proteins in human milk is considered not fully nutritionally available to the infant until 6 weeks postpartum [101]. It has been proposed that urea can be salvaged via breakdown in the colon, incorporated into microbial proteins, and release as amino acids that can be absorbed by gut epithelial cells and utilized for host metabolism. Since *Bifidobacterium* are predominant gut colonizers in newborns, it is particularly significant that these microbes are capable of degrading urea and thereby aiding nitrogen recycling to the host. Historically, very limited studies have focused on urease function in *Bifidobacterium*. The underlying mechanisms of this process are poorly understood. This current study serves as a starting point for future analysis regarding bifidobacterial urease and its potential impacts on infant health and early development.

The *ureC* amino acid sequence aligned among bifidobacterial strains from 12 subspecies indicates a very high similarity (data not shown). Among the genus of *Bifidobacterium*, only some species, (*B. aesculapii*, *B. biavatii*, *B. callitrichos*, *B. infantis*, *B. kashiwanohense*, *B. suis*, *B. scardovii*, *B. subtilis*) harbor a complete urease gene cluster including a urea transporter, a nickel transporter, urease alpha and beta/gamma subunits, and urease accessory proteins. Interestingly, many of the species were isolated from human infant or non-human primates including baby common marmoset and cotton-top tamarins (data not shown). The *B. suis* strain UMA399 in this study was isolated from a rhesus macaque infant. Some other *Bifidobacterium* species such as *B. bifidum* only contain one urea transporter gene on its genome, which may be the result of gene horizontal transfer during adaptation to the host or environment. As human milk provides the first and sole nutrient for infant, whether human milk urea is an evolutionary retention force for urease genes within bifidobacterial species still needs further discussion.

In this study, urease activity was detected among several bifidobacterial strains including *B. infantis*, *B. suis*, and *B. longum* strains. A diversity of urease activity was also detected from complex nitrogen, 2% urea, and 2% urea plus Ni²⁺ as the growth media. Notably, *B. suis* UMA399 exhibits a very strong activity even in complex nitrogen, which is consistent with a previous study [82]. However, contrary to another previous study [81], we found that urease in bifidobacteria is significantly elevated by urea and nickel compared to its basal expression in complex nitrogen. Nickel, as the cofactor of urease, its function has been widely studied in many bacterial ureases. As we predicted the protein structure of the wild-type UreC, the model gave a structure with Ni²⁺ niche similar to the known structures. While nickel detected from our growth medium is only in trace amounts (data not shown), its presence has been identified in human milk during lactation, differentiating between individuals [102-105]. As we detected, a concentration of 50 µM Ni²⁺ elevated the urease activity in *Bifidobacterium*. The existence of nickel in human milk might be a potential stimulator for urease function. Targeted mutagenesis has been performed on many bacterial urease genes e.g., *H. pylori* etc. In this study, we screened a mutant from *B. suis* UMA399, its *ureC* was knocked out by chemical mutagenesis. However, our study suggested that the substitution of the key residue - 343 Glutamine affects the maturation of an active urease, resulting a configuration difference and deficient urease activity.

Transformation is an essential technique for functional analyses of genes in bacteria. So far, the transformation efficiency in the genus of *Bifidobacterium* is still generally low, with a median efficiency of 10³ CFU per µg plasmid DNA mainly by electroporation [34]. The electro-transformation protocols developing for bifidobacteria still require strain-dependent methodology [31]. To the best of our knowledge, there are no other reports of *Bifidobacterium longum* subsp. *suis*

transformation. The shuttle vector used in this study, pDOJHR, has been previously used in *B. longum* [26]. Accordingly, our transformation employed for the *B. suis* UMA399 mutant strain was optimized using pDOJHR. Key experimental conditions for this transformation included using mid-logarithmic-phase cells ($OD_{600\text{ nm}} = 0.4 - 0.6$), a washing buffer with high-amount sucrose (0.5 M), and a 30 - min preincubation before the electric pulse (25 μ F, 200 Ω , 2.2 kV), which is widely used in most recent studies on bifidobacteria. Interestingly, we found that using just plain MRS as the growth and recover medium, without extra carbohydrates, gave an adequate transformation efficiency ($\sim 10^2$ CFU per μ g DNA). Although other methods include adding high concentrations of sugars (sucrose, raffinose, fructo-oligosaccharides etc.) into the growth medium [24, 26, 29, 32], our result suggested that extra sugar might not be essential under every circumstance. Previous researchers have successfully created bifidobacteria mutants using plasmid artificial modification techniques. The PAM method has shown its efficacy in a few strains including *Bifidobacterium adolescentis* ATCC15703 and *Bifidobacterium breve* UCC2003. As there is still a barrier for making a targeted mutation in our strain, EMS mutagenesis was used in this study to make the urease mutation. Since EMS mutagenesis is random, the odds of creating the desired gene mutation are very low. A more applicable and wild-spectrum genetic tool for inducing gene mutations is essential for future bifidobacterial research.

3.5 Conclusions

To our knowledge, this is the first study on bifidobacterial urease gene function. We demonstrated that the E343K mutation on the UreC lead to configuration and functional change, which impedes its catalyzing activity during the hydrolysis of urea. Thus, UreC is essential for the bifidobacterial urea utilization phenotype. This further adds to scientific knowledge regarding host-microbiome interaction catalyzed by

human milk.

3.6 Acknowledgements

The authors thank Cindy Kane for technical assistance and various members of the UMass Amherst Food Science department for their support. We acknowledge Dr. Daniel J. O' Sullivan (University of Minnesota) for providing pDOJHR and Dr. Margaret Stratton (University of Massachusetts Amherst) for providing pSMT3 and the SUMO protease. We thank Dr. Nathaniel Howitz for advice and guidance throughout the project. This research has been funded in part through a grant from the U.S. Department of Agriculture (2016-67017-24425).

3.7 Author contributions

YL and DAS designed the study. YL performed the experiments, interpreted the data, and drafted the manuscript through several iterations. DW facilitated whole genome sequencing KA analyzed the raw data from whole genome sequencing, optimized the protocol for variation analysis, and critically reviewed the manuscript. LD helped with ICP-MS analysis on nickel-binding of the wild-type UreC and the mutant UreC. DAS conceived the study, revised, and approved the manuscript.

CHAPTER 4

EXPLORING L-CYSTEINE AUXOTROPHY IN BIFIDOBACTERIUM

4.1 Introduction

Cysteine and methionine are the two proteinogenic and sulfur-containing amino acids that are essential for bacteria [106]. Specifically, cysteine has been used in bifidobacterial culture as a necessary growth supporter as well as an redox potential reducer [107]. Cysteine has been found in human milk as one of the free amino acids [108], as well as in human intestines as a metabolite from the gut microbes [109].

Previous studies found that many species of *Bifidobacterium*, including *B. infantis*, *B. bifidum*, *B. breve* are cysteine auxotrophic, in which cysteine biosynthesis pathways are inactive. Pathways of cysteine and methionine biosynthesis have been well clarified in *E. coli*.

There are two cysteine biosynthesis pathways. In the first pathway, cystathionine beta-synthase (CBS) converts serine and homocysteine (a product of methionine degradation) to form cystathionine in an irreversible reaction. The cystathionine is then degraded by cystathionine gamma-lyase (CGT) to cysteine. In the other pathway, serine is converted to O-acetyl-serine by serine acetyltransferase (*cysE*). With the incorporation of hydrogen sulfide, and catalysis of cysteine synthase (*cysK*), O-acetyl-serine is converted to cysteine and acetate [110].

For *Bifidobacterium*, the cysteine/methionine biosynthesis pathways are poorly characterized. Most bifidobacterial strains behaves cysteine prototrophic, including *B. infantis*, *B. bifidum* [111-113]. However, cysteine auxotrophy is not a common feature of all the species in the genus *Bifidobacterium*. Representatives of some species such as *B. boum*, *B. minimum*, *B. pullorum*, *B. ruminantium*, *B. saguini* and *B. scardovii*

showed slightly growth without adding cysteine [113]. The cysteine auxotroph is mainly due to the lack of key enzymes in its biosynthesis pathways. In *Lactobacillus*, the function of *cysE*, and *cysK* needed for cysteine synthesis from serine was confirmed by complement the *E. coli cysE* and *cysK* mutants. [110, 114]. For *Bifidobacterium*, studies on cysteine auxotrophy are very limited. The only report on the cysteine auxotrophic behavior is on *B. bifidum* PRL2010. Results indicated that genes needed for sulfate transport and reduction to sulfide are lacking, which is common in *Bifidobacterium* [115]. The transcription of genes involved in cysteine and methionine metabolism was not stimulated by the access of these amino acid residues. For other bifidobacterial (sub) species such as *B. infantis*, its cysteine auxotrophic behavior has not been characterized. *B. infantis* is predominant constituent in the infant gut due to their capacity growth on human milk oligosaccharides. It will be important to investigate how *B. infantis* utilizes cysteine and its nutrients requirement to further revealing its role in the infant gut during their early development.

In this chapter, we investigated the auxotrophic behavior of *Bifidobacterial* strains, by comparing to some cysteine prototrophic strains of the species *B. boum*. We performed *in silico* analysis on genes involved in their cysteine and methionine metabolism together with transcription level quantification. Grow assay in variant nitrogen sources was monitored to clarify the phenotypes related with cysteine utilizations.

4.2 Material and Methods

4.2.1 Bacteria and Culture Conditions

B. infantis UMA272, *B. suis* UMA399, *B. scardovii* JCM12489, *B. boum* LMG 10736, will be used for this study. Single colonies of bifidobacteria were grown overnight in De Man-Rogosa-Sharpe (MRS) broth (Difco, USA) supplemented with

0.05% (wt/v) L-cysteine and incubated overnight at 37°C in a Coy anaerobic chamber (Coy Laboratory Products, MI) with an atmosphere of 90% N₂, 5% CO₂ and 5% H₂.

4.2.2 Construction of the *CysK* and *MetB* Expression Vector

The *E. coli-Bifidobacterium* shuttle vector pDOJHR was used for this study. The 195 bp upstream and 60 bp downstream region flanking the cystathionine beta-synthase (EC 4.2.1.122) (*cysK*) and cystathionine gamma-lyase (EC 2.5.1.48) (*meB*) coding sequence (CDS) from the genome of *B. suis* UMA399 was amplified by primer CYS-F/R, in which *EcoRI* sites were incorporated. The amplicon and pDOJHR were digested with *EcoRI*, ligated by T4 DNA ligase (NEB, USA), and transferred to *E. coli* strain NEB 5-alpha (NEB, USA). The insert within the plasmid was confirmed by sequencing at Eton Bioscience (Boston, USA) to make sure that there is no mutation. The pDOJHR vector with the *cysK* and *metB* gene was named pDOJ-cysK-metB, as shown in **Figure A5** drawn by SnapGene (from GSL Biotech; available at snapgene.com).

4.2.3 Electroporation

A 5% (v/v) overnight culture of the *B. infantis* UM272 strain was used to inoculate 40 mL MRS (Difco, USA) supplemented with 0.05% L-cysteine and incubated at 37°C until an OD_{600 nm} of 0.4-0.5 was reached. Cells were collected at 4,696 × g for 15 min at 4°C, then washed 3 times with 30 mL ice-cold electroporation buffer [10% (v/v) glycerol and 0.5 M sucrose]. Cells were resuspended in 1 mL buffer in a microcentrifuge tube, pelleted again, and resuspended in 1/250 (v/v) of the original culture. For each transformation, 50 µL of the cell suspension and 400 ng of plasmid DNA were mixed and incubated on ice for 30 min, then transferred to a pre-chilled 1 mm disposable cuvette. A voltage electric pulse was delivered through a Gene Pulser (Bio-Rad) at 25 µF, 200 Ω and 2.2 kV. Cells were immediately resuspended with 950

μL of MRS (Difco, USA), transferred into a 15 mL falcon tube, and recovered anaerobically for 3 hours at 37°C. After which, cells were diluted and plated on aluminum foil-wrapped MRS plates supplemented with 5 $\mu\text{g mL}^{-1}$ chloramphenicol and incubated anaerobically at 37°C for 48-72 h. Plasmid isolation from bifidobacteria transformants was optimized from Francesca *et al.* [92].

4.2.4 Growth Dependence on Nitrogen and Sulfur Source

The growth phenotype of cells in variant nitrogen sources was monitored in a 96-well plate. Cells from overnight MRS broth culture were used to inoculate at 1% (v/v) into a basal medium adding 0.2% urea, 0.02%-0.05% glutamine, cysteine or methionine as the sole nitrogen source. The base medium contained 2% D-glucose, 0.2% potassium phosphate dibasic anhydrous, 0.5% sodium acetate anhydrous, 0.02% magnesium sulfate heptahydrate, 0.005% manganese (II) sulfate monohydrate, 0.1% Tween 80. The basal medium with 1% peptone, 0.8% yeast extract, 0.1% ammonia citrate and 0.05% L-cysteine was regarded as a positive control; The basal media that only contained carbon source was regarded as negative control. The growth assay was conducted at 37°C for up to 28 hours in a microplate spectrophotometer (BioTek, USA) placed within the anaerobic chamber. Reads were performed with shaking at intervals of 5 min to detect optical density at 600 nm. Each strain was measured in biological triplicate with three technical repeats. For growth with various sulfur compounds, the 0.02% magnesium sulfate heptahydrate and 0.005% manganese (II) sulfate monohydrate in the basal medium were replaced by 0.02% magnesium chloride hexahydrate and 0.005% manganese (II) chloride tetrahydrate respectively. The new basal medium containing either 0.05% methionine or 0.05% methionine plus 0.7 mM sodium or both was inoculated with *B. boum* LMG10736 (1% v/v). Basal medium with sulfur source excluded was used as negative control.

4.2.5 Mutant generation by Ethyl methane sulfonate (EMS)

Bifidobacterial cells from a 4 mL of overnight culture were spun down and resuspended in 4.75 mL phosphate buffer [pH7.2]. A 250 μ L of EMS (99%) was added to reach a final concentration of 5% (v/v). The mixture was incubated at 37°C for 30 min. Cells were pelleted again and washed 3 times with fresh MRS. Cell suspension in 5 mL fresh MRS was diluted to 25% of the original concentration and grown overnight. Dilutions of 100 μ L overnight mutagenized cultures were spread on a cysteine prototroph selective agar. The selective agar was made from a base agar (2% D-glucose, 0.2% potassium phosphate dibasic anhydrous, 0.5% sodium acetate anhydrous, 0.02% magnesium sulfate heptahydrate, 0.005% manganese (II) sulfate monohydrate, 0.1% Tween 80) supplemented with 0.1% methionine. The base agar was used as negative control. The basal agar with 1% peptone, 0.8% yeast extract, 0.1% ammonia citrate and 0.05% L-cysteine was regarded as a positive control; Plates were incubated anaerobically at 37°C for 2 weeks.

4.2.4 Multiple Sequence Alignment

The protein sequences of the cystathionine beta-synthase (EC 4.1.2.22) were retrieved from Integrated Microbial Genomes (IMG) in DOE Joint Genome Institute (JGI; <http://img.jgi.doe.gov>). Multiple alignment was visualized by the Geneious Prime 2019. 2.1. (<https://www.geneious.com>)

4.2.5 Distribution of cysteine and methionine biosynthesis genes in *Bifidobacterium*

Heatmaps were generated by pheatmap RStudio Team (2018). RStudio: Integrated Development for R. RStudio, Inc., Boston, MA URL <http://www.rstudio.com/>. Each gene count was retrieved from the PATRIC- version 3.5.30 Comparative Pathway Service (Wattam, 2016). Cysteine and methionine

biosynthesis pathways were referred to *E. coli* and *Bacillus subtilis* from MetaCyc (<http://metacyc.org>) [116].

4.2.6 Statistical Analysis

All analyses were performed with GraphPad Software Prism 8.0.1 (GraphPad Software, Inc., CA, USA). Results were shown as mean \pm standard deviation (*SD*). The models were checked for normality and variance homogeneity and data transformation was performed when necessary and was analyzed through one-way analysis of variance (ANOVA) followed by Tukey's multiple comparison test. $P < 0.05$ was classified as significant.

4.3 Results

4.3.1 UMA272, UMA399 and JCM12489 are cysteine auxotrophic strains.

To evaluate the utilization of cysteine, methionine and 2% urea as the sole nitrogen source by *B. infantis* UMA272, *B. suis* UMA399 and *B. scardovii* JCM12489, we measured their growth in the corresponding culture as shown in **Figure 12**. Panel A shows that *B. suis* UMA399 was not able to utilize 2% urea as a sole nitrogen source compared to the control, when adding cysteine, it grew significantly higher. Panel B shows that *B. infantis* UMA272, *B. suis* UMA399 and *B. scardovii* JCM12489 did not grow in methionine compared to the negative control. Only when cysteine was added in growth medium, a significant higher growth was observed. The addition of methionine to cysteine promoted growth compared to that in cysteine as the sole nitrogen source. This interestingly suggested that these bacterial strains are only able to use methionine when cysteine is in the medium.

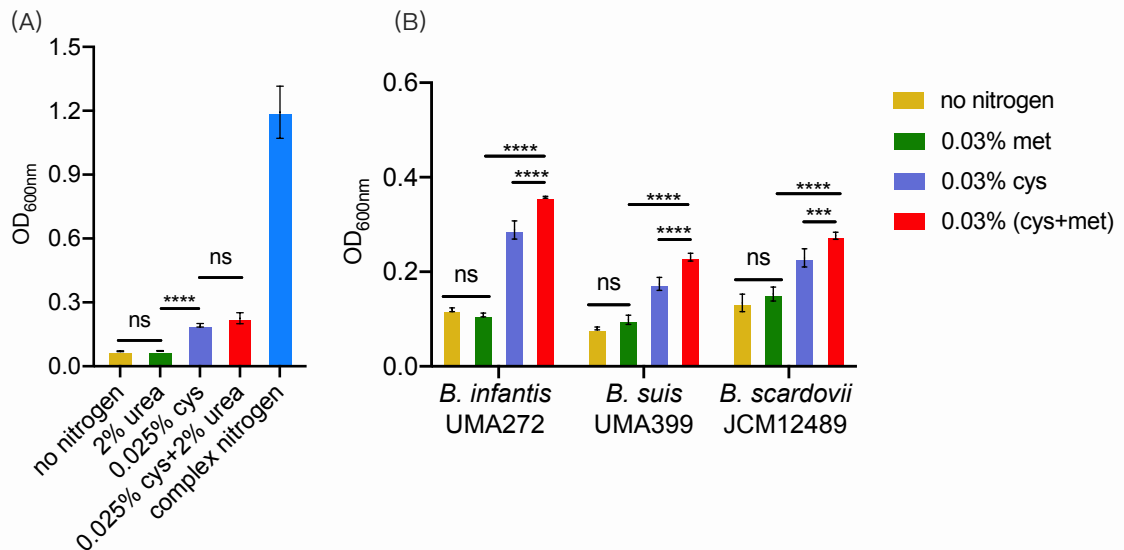


Figure 12 Growth phenotype of *B. infantis* UMA272, *B. suis* UMA399 and *B. scardovii* JCM12489 in cysteine and methionine and urea.

Panel A: *B. suis* UMA399 utilization of urea. Panel B: *B. infantis* UMA272, *B. suis* UMA399 and *B. scardovii* JCM12489 utilization of cysteine and methionine. The bars display the final optical density at 600 nm by mean \pm SD (standard deviation) from three individual biological replicates (n = 3). cys, cysteine; met, methionine; cys + met, cysteine + methionine. NS (not significant; $P > 0.05$), **** $P < 0.0001$.

4.3.2 Truncated CysK and MetB in UMA272 is not responsible for cysteine auxotrophy

As we were compared the genes related with cysteine biosynthesis in variant bifidobacterial strains, we found that the protein sequence of cystathionine beta-synthase (EC 4.2.1.22) (*cysK*) and gamma-lyase (EC 2.5.1.48) (*metB*) genes in *B. infantis* UMA272 are truncated as shown in **Figure 13** (first sequence from the top). Except for UMA272 and UMA399, all other strains were tested to be cysteine prototroph [117]. Growth results showed that *B. infantis* UMA272 and *B. suis* UMA399 were both cysteine auxotroph, even though the cystathionine *cysK* and *metB* genes in UMA399 were of highly similar to the other cysteine prototrophic strains. However, for UMA272, both its *cysK* and *metB* genes were truncated (data only shown). To figure

out if the truncated *cysK* and *metB* genes lead to the cysteine auxotrophy of UMA272, we cloned the cystathionine *cysK* and *metB* genes from UMA399 into the shuttle vector pDOJHR (pDOJ-cysK-metB), transferred it into UMA272, and tested the growth of UMA272 with and w/o the pDOJ-cysK-metB in cysteine and methionine. Results in **Figure 14** shows that *B. infantis* UMA272 with pDOJ-cysK-metB was not able to grow in methionine as the sole nitrogen source compared to the negative control. This suggested that other pathways or gene regulations besides the expression of cystathionine beta-synthase (EC 4.2.1.22) and gamma-lyase (EC 2.5.1.48) might be needed to enable cysteine biosynthesis in *B. infantis* UMA272.

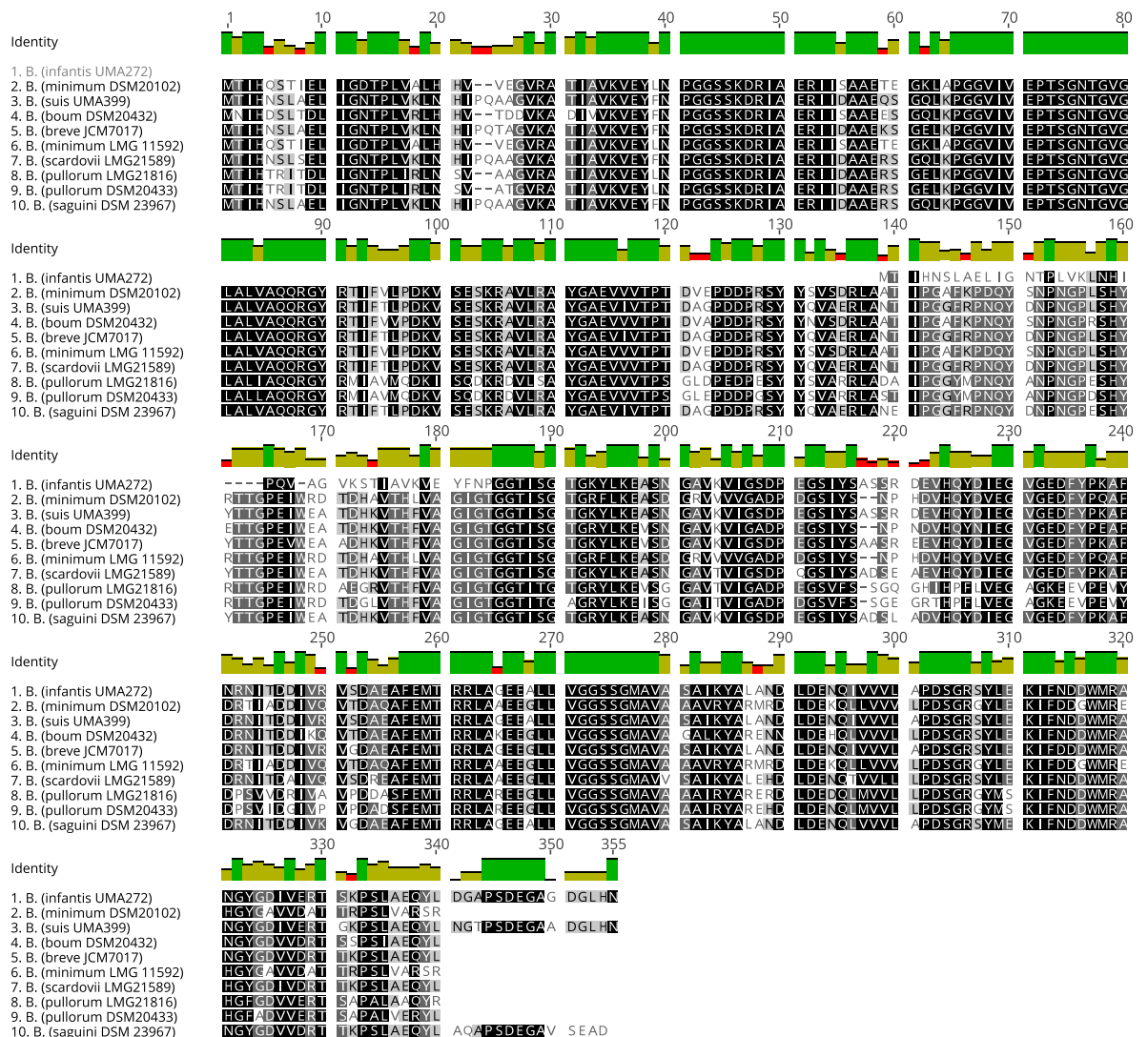


Figure 13 Multiple alignment of cystathionine beta-synthase (EC 4.2.1.22) protein sequence in variant species of *Bifidobacterium*.

Sequence similarity is indicated by green, olive and red bar chart. (Green: 100% identity; Olive: 30% - 100% identity; Red: less than 30% identity). Conserved to non-conserved residues are highlighted by black, dark grey, light grey and white. (Black: 100% similar; dark grey: 80% - 100% similar; Light grey: 60% - 80% similar; White: less than 60% similar). The strains from up to down are: *B. infantis* UMA272, *B. minimum* DSM20102, *B. suis* UMA399, *B. boum* DSM20432, *B. breve* JCM7017, *B. minimum* LMG11592, *B. scardovii* LMG21589, *B. pullorum* LMG21816, *B. pullorum* DSM20433, *B. saguini* DSM23967.

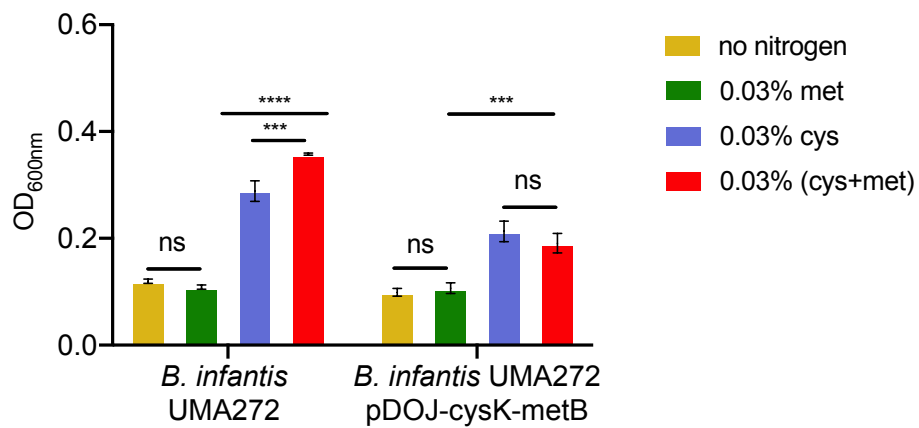


Figure 14 Growth phenotype of *B. infantis* UMA272 with or without pDOJ-cysK-metB in cysteine and methionine.

The bars display the final OD_{600 nm} by mean \pm SD (standard deviation) from three individual biological replicates (n = 3). cys, cysteine; met, methionine; cys + met, cysteine + methionine. pDOJHR-cysK-metB, pDOJHR carrying the cystathionine beta-synthase (EC 4.2.1.22) and gamma-lyase (EC 2.5.1.48) genes from *B. suis* UMA399. NS (not significant; $P > 0.05$). *** $P = 0.0002$, **** $P < 0.0001$.

4.3.3 LMG10736 is a cysteine prototroph

Utilization of cysteine, methionine and glutamine by *B. boum* LMG10736 is shown in Figure 15. This strain grew in both sulfur-containing amino acids cysteine and methionine. Its growth in glutamine as a sole nitrogen source was not significant.

This confirmed that *B. boum* LMG10736 is a cysteine prototroph as it can use methionine as a sole nitrogen source for its growth.

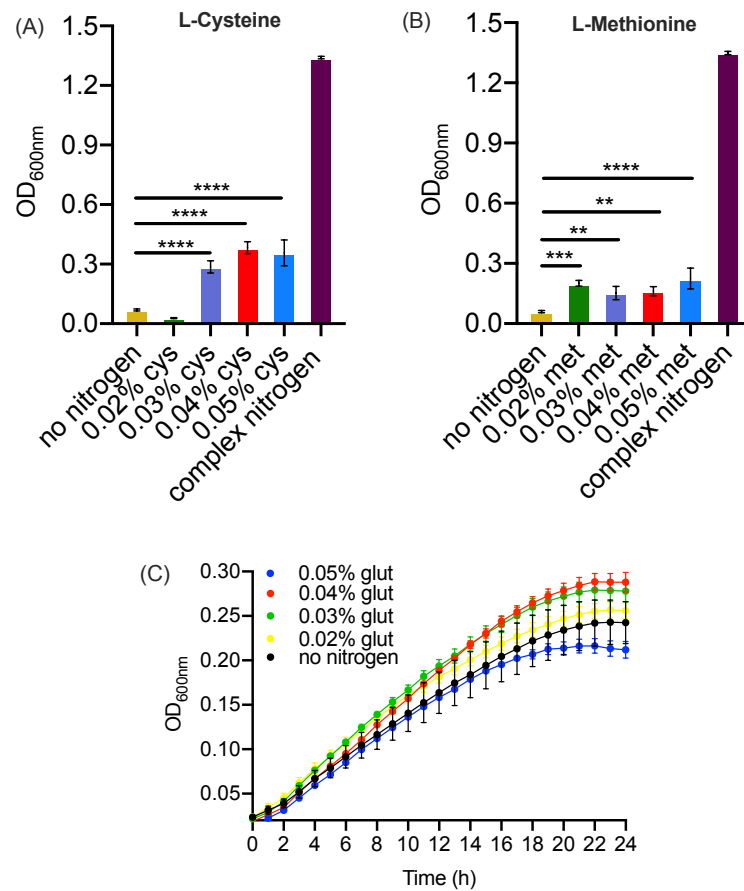


Figure 15 Growth phenotype of *B. boum* LMG 10736 in L-cysteine, methionine and glutamine.

B. boum LMG10736 was cultured in 0.02-0.05% cysteine (panel A), methionine (panel B), glutamine (panel C). The bars display the final OD_{600 nm} by mean \pm SD (standard deviation) from three individual biological replicates (n = 3), analyzed by 2way ANOVA followed by Tukey's multiple comparison test (** P = 0.0021, *** P = 0.0002, **** P < 0.0001). The continuous growth curve of *B. boum* LMG10736 in glutamine shows optical density at 600 nm at each time point by mean \pm SD (standard deviation) from three individual biological replicates (n = 3). cys, cysteine; met, methionine; glut, glutamine.

4.3.4 LMG10736 can utilize methionine as both nitrogen and sulfur source but cannot utilize *in vitro* sulfate or sulfide as sulfur source.

The predicted biosynthesis pathway of cysteine and methionine needs the incorporation of sulfide at certain steps as shown in **Figure 17**. In bacterial cells, sulfide can be obtained by reducing sulfate, as well as from degradation of sulfur-containing amino acids, such as cysteine or methionine. To test if methionine can be utilized by *B. boum* LMG10736 as a sulfur source, we replaced the MnSO_4 and MgSO_4 with MnCl_2 and MgCl_2 , added methionine as the sole nitrogen and sulfur source. Meanwhile, we also added sulfide in addition to methionine to see if the *in vitro* sulfide would stimulate the growth of LMG10736. Results in **Figure 16** shows that *B. boum* LMG10736 was not able to utilize sulfide as a sulfur source, as it exhibited a much lower growth compared to 0.05% methionine. Compared to the group without nitrogen and any sulfur, the control group without nitrogen that contained sulfates in the growth medium did not show significant growth neither, indicating that *B. boum* LMG10736 was not able to utilize sulfates besides sulfide. While in 0.05% methionine as both nitrogen and sulfur source, *B. boum* LMG10736 grew the best. This confirmed the sulfur containing amino acid methionine is incorporated into sulfur metabolisms.

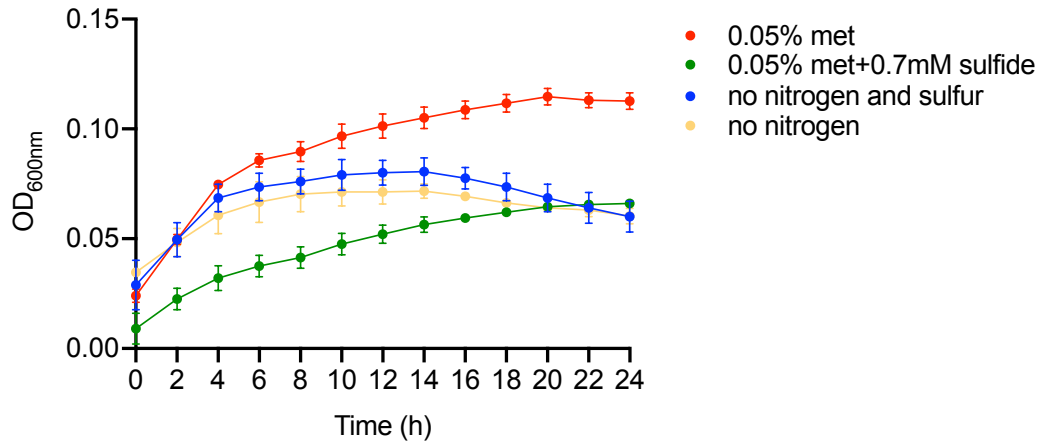
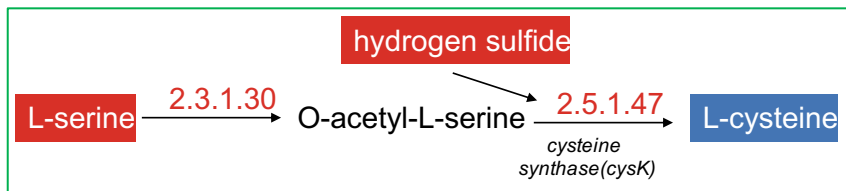


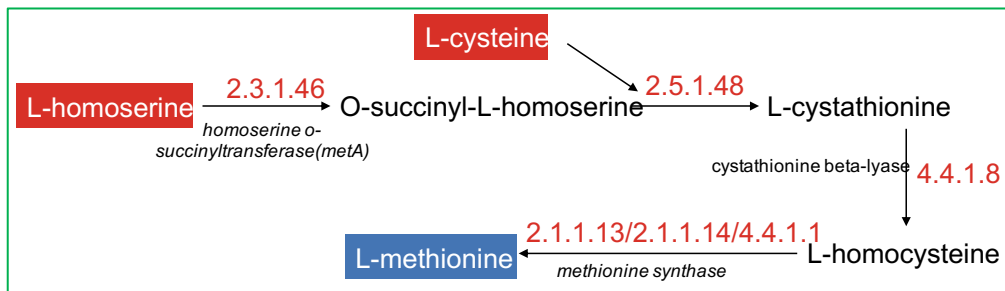
Figure 16 Growth phenotype of *B. boum* LMG 10736 in modified medium that contained sulfur containing amino acids or sulfide.

B. boum LMG 10736 was cultured in 0.05% methionine, 0.05% methionine with 0.7mM sulfide. The growth curves display the optical density at 600 nm by mean \pm *SD* (standard deviation) from three individual biological replicates (n = 3).

(A)



(B)



(C)

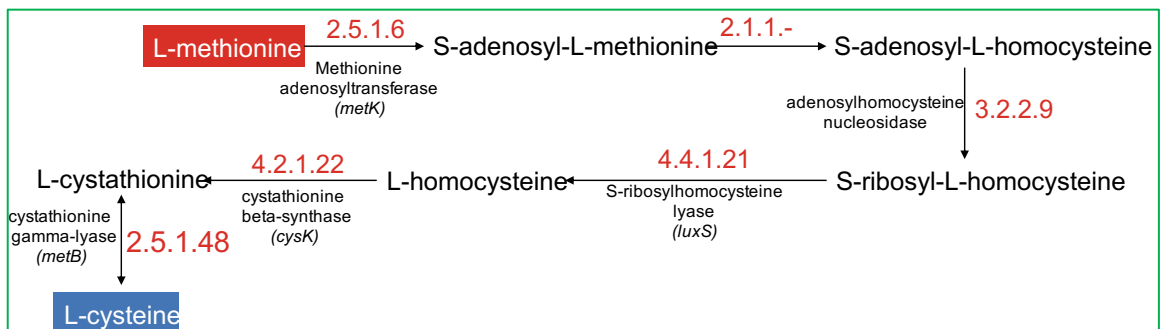
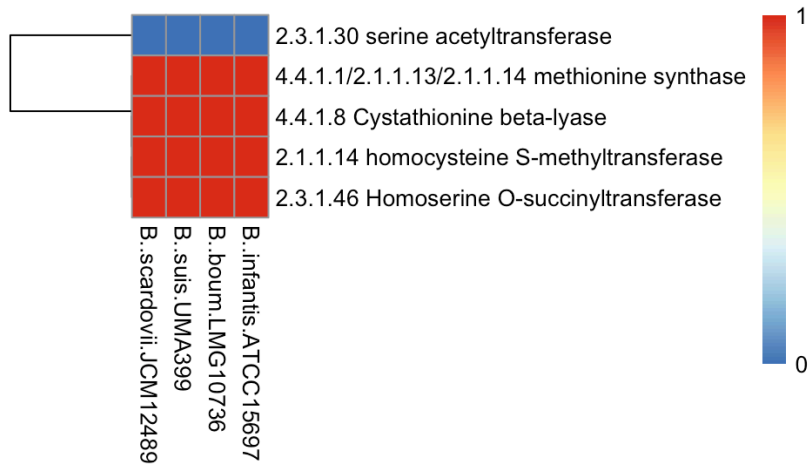


Figure 17 Predicted pathways of cysteine and methionine biosynthesis in *Bifidobacterium*.

Red marked the start/key metabolite in each pathway. The blue boxes marked the end metabolite in each pathway. Arrows shows the direction of reactions, connecting each middle metabolite. EC number of the enzyme in each reaction is marked in red with description and gene symbol below.

(A)



(B)

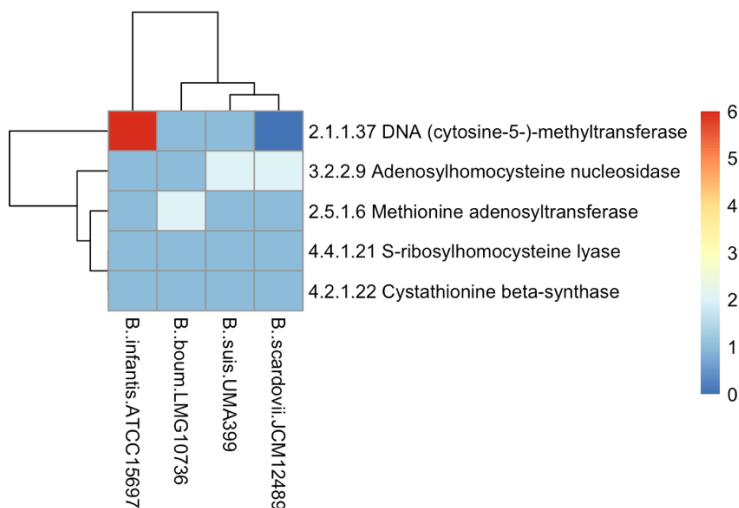


Figure 18 Distribution of cysteine and methionine biosynthesis genes in *B. infantis* UMA272 (ATCC15697), *B. suis* UMA399, *B. boum* LMG10736, *B. scardovii* JCM12489.

The legend scale on the right indicate the gene counts found on the genome. Red: 6, Light blue: 2; Dark blue: 1; Navy: 0. Y axis shows the participated enzymes with EC number; X axis shows the strain names.

4.3.5 Predicted cysteine biosynthesis pathways in bifidobacterial strains

The predicted biosynthesis pathways of cysteine and methionine is shown in **Figure 17**, and the distribution of genes participated in these pathways on bifidobacterial genomes is shown in **Figure 18**. According to prediction, cysteine can

be directly synthesized from serine (**Figure 17A**) or from methionine degradation (**Figure 17C**). For the serine pathway, the enzyme - Serine acetyltransferase (EC 2.3.1.30) is missing in all these four strains (**Figure 18A**). *B. infantis* UMA272 (ATCC15697), *B. suis* UMA399, *B. scardovii* JCM12489 are cysteine prototroph as confirmed previously. Interestingly, all these bifidobacterial strains except for *B. scardovii* JCM12489 were found to contain all the genes for the methionine degradation pathway on their genomes (**Figure 18B**). For methionine biosynthesis pathway, the incorporation of cysteine is a necessity.

4.4 Discussion

For *Bifidobacterium*, the mechanisms underlying cysteine auxotrophy are poorly understood. This study tested several bifidobacterial strains including *B. infantis* UMA272, *B. suis* UMA399, and *B. scardovii* JCM12489, *B. boum* LMG10736. on their ability to utilize non-cysteine sole nitrogen sources, as well as sulfur sources. Cysteine and methionine are two sulfur-containing, proteinogenic amino acids, which are essential for bacterial growth. The cysteine/methionine biosynthesis pathway has not been clarified in the genus of *Bifidobacterium*. In this study, we combined growth test and genomic analysis to provide putative interpretations to the auxotrophic behavior in *Bifidobacterium*.

To analyze the cysteine/methionine biosynthesis genes in these bifidobacterial strains, we referred to the similar pathways from well-studies bacterial strains including *E. coli* and *Bacillus subtilis*. For cysteine synthesis, we first checked the pathway in which serine is synthesized to cysteine. Since the first reaction enzyme is missing, we then predicted this pathway is not functional. The missing of serine pathway was also found in many other bifidobacterial strains as we checked their genome (data not shown).

Cysteine may also be produced by methionine degradation. We found that genes in this pathway are existing in *B. infantis* UMA272, *B. suis* UMA399 and *B. boum* LMG10736. As we identified, *B. infantis* UMA272 has a truncated cystathionine beta-synthase (EC 4.2.1.22) (cysK) and cystathionine gamma-lyase EC 2.5.1.48 (metB) but is not the only reason for its auxotrophic behavior. In contrast, *B. suis* UMA399 has complete genes for every enzyme (data not shown) similar to the prototrophic strain *B. boum* LMG 10736 but is still cysteine auxotrophic. Thus, we predicted that for UMA272 and UMA399, their auxotrophic behavior can be related with gene silencing on the methionine degradation pathway on transcriptional or translational level. For, *B. scardovii* JCM12489, the missing of DNA (cytosine-5-)-methyltransferase might be the reason for its auxotrophic behavior.

As we found, sulfur metabolisms are along with the biosynthesis sulfur-containing amino acids cysteine and methionine. Many bacteria can obtain sulfide from sulfate reduction. However, this is a rare phenotype in *Bifidobacterium*. The cysteine prototrophic strain *B. boum* LMG10736 did not show utilization of either sulfate or sulfide and no sulfur transport system was found on its genome (data not shown). This indicated that *B. boum* LMG10736 probably utilized the organic sulfur that from the backbone of methionine to synthesize cysteine and support its growth. The absence of sulfur transport and reduction to sulfide is common in *Bifidobacterium* [115], as was also found in *B. bifidum* PRL2010. The missing of these genes in *Bifidobacterium* might be related with adaption to the specific niche. Whether there is an absorbance of non-organic sulfur sources (sulfides, sulfates) or organic sources (cysteine, methionine) by *Bifidobacterium* from the surrounding environment and gut commensals deserves future investigation.

4.5 Conclusions

This study provides initial insights for cysteine auxotrophic behavior in some bifidobacterial species. Future work on transcriptomics, proteomics or metabolomics is still needed to depict the complete cysteine and methionine biosynthesis pathway in *Bifidobacterium*. This preliminary data may also open a new avenue of research for understanding how auxotrophic gut commensals may acquire essential nutrients from the gut environment.

CHAPTER 5

FUTURE WORK

In chapter 3, the bifidobacterial urease function was investigated by characterizing a *ureC* mutant generated from *Bifidobacterium long* subsp. *suis* UMA399. The protein structural analysis of the wild-type UreC and the mutant UreC can be further analyzed in the future. First part will be crystallization of both UreC accompanied by detailed protein structure analysis by protein mass spectrometry. The wild-type UreC and the mutant UreC incubated with N^{2+} showed a configuration difference that may be related with nickel-binding. To deeply explain the configuration difference, inductively coupled plasma mass spectrometry (ICP-MS) can be applied to further test how much nickel ions each protein can bind to, which will evaluate the nickel-binding ability between the wild-type UreC and the mutant UreC.

It is also interesting to study how urea utilization will impact the infant gut microbial community dynamics, as well as the profile of metabolites. For this purpose, a bioreactor system simulating the fermentation of gut environment can be used. Bacteria isolated from infant fecal samples can be incubated with the growth culture supplemented with urea in the bioreactor for tracking growth. Metabolites in the culture from the bioreactor can be sent for HPLC analysis. 16S rDNA sequencing can be conducted on bacteria from the infant fecal samples as well as various fermentation point to check the bacterial community dynamics.

In addition, a targeted mass spectrometry-based metabolic profiling study can also be performed to study urea salvaging in animal model. Blood samples will be taken from the germ-free mice inoculated with bifidobacteria and fed with a designed diet

supplemented with isotope-labelled urea. MS-based equipment will be used to identify the plasma protein from the plasma to track urea salvaging.

In chapter 4, the cysteine auxotrophic behavior in bifidobacterial strains was explored based on growth assay and genomic analysis. It is also important to study the transcriptional level change of cysteine/biosynthesis genes either by qRT-PCR or by RNAseq. For higher-quality RNA extraction, a chemically defined medium that contains every single amino acid with exclusion of methionine or cysteine will be useful to increase bacterial growth and cell mass. Total RNA will be extracted from bifidobacterial cells cultured from cysteine, methionine or both. Putative genes in cysteine and methionine biosynthesis pathways including *metA*, *metB*, *metC*, *metC*, *metE*, *cysE*, *cysK* can be targets to test their expression level change corresponding to the nitrogen source.

In addition to transcriptional level, a proteomic experiment can also be performed to verify the protein profiles associated with cysteine biosynthesis. Bifidobacterial strains that are cysteine prototrophic can be grown in isotope-labeled methionine as a sole nitrogen source. Cell free lysate can be extracted from the cells to identify where the labeled methionine is incorporated into in the pathways that synthesizing cysteine, such as the methionine degradation pathway. Products in the middle of the reaction can also be detected to depict a concise cysteine/biosynthesis pathway for *Bifidobacterium*.

APPENDIX

SUPPLEMENTARY TABLES AND FIGURES

Table A1. Bacterial strains, plasmids and primers used in this study.

UMA, University of Massachusetts Amherst Culture Collection. In primers, start

codon and stop codon are underlined; restriction sites are indicated in lowercase.

Strains	Genotype and relevant features	Source
<i>Bifidobacterium</i> strains		
<i>B. longum</i> subsp. <i>infantis</i> UMA272	Isolate from infant feces	This study
<i>B. longum</i> subsp. <i>infantis</i> UMA302	Isolate from infant feces	This study
<i>B. longum</i> subsp. <i>infantis</i> UMA299	Isolate from infant feces	This study
<i>B. longum</i> subsp. <i>longum</i> UMA306	Isolate from human feces	This study
<i>B. longum</i> subsp. <i>suis</i> UMA399	Isolate from infant rhesus macaque feces	This study
<i>B. scardovii</i> JCM12489	Isolated from human blood	JCM
<i>B. boum</i> LMG10736	Isolated from bovine rumen	JCM
<i>E. coli</i> strains		
Rosetta (DE3)	F ⁻ <i>ompT hsdS_b</i> , (rB ⁻ mB ⁻) <i>gal dcm</i> (DE3) pRARE (Cm ^r)	This study
NEB 5-alpha	<i>fhuA2 Δ(argF-lacZ)U169 phoA glnV44 Φ80Δ (lacZ)M15 gyrA96 recA1 relA1 endA1 thi-1 hsdR17</i>	New England Biolabs
Plasmids		
pSMT3	5.8-kb, <i>E. coli</i> expression vector, encoding an N-terminal, Ulp1-cleavable 6xHis-Sumo tag, Kan ^r	[120]
pSMT-U	pSMT3 carrying the wild-type or mutant <i>ureC</i>	This study
pDOJHR	8.5-kb, <i>E. coli-Bifidobacterium</i> shuttle vector, Cm ^r	(Lee & O'Sullivan, 2006)
pDOJ-U	pDOJHR carrying the wild-type <i>ureC</i>	This study
pDOJ-cysK-metB	pDOJHR carrying the <i>cyK</i> and <i>metB</i> from UMA399	This study
Primers		
PSM-F	5'-gctaggatcc <u>ATGAAGATTATTACGC</u> -3'	This study
PSM-R	5'-tcgtctcgag <u>TCAGAACAGGAAGTAC</u> -3'	This study
PD-F	5'-taacgaattcTGTGAGGTTTCGAGC-3'	This study
PD-R	5'-gagcgaattcCATTTCGTGACCGAA-3'	This study
CYS-F	5'-TGAGgaattcCGTGGTTAACATGA-3'	This study
CYS-R	5'-TAATgaattcGAGTCCGCCGATAA-3'	This study

JCM, Japan Collection of the Microorganisms.

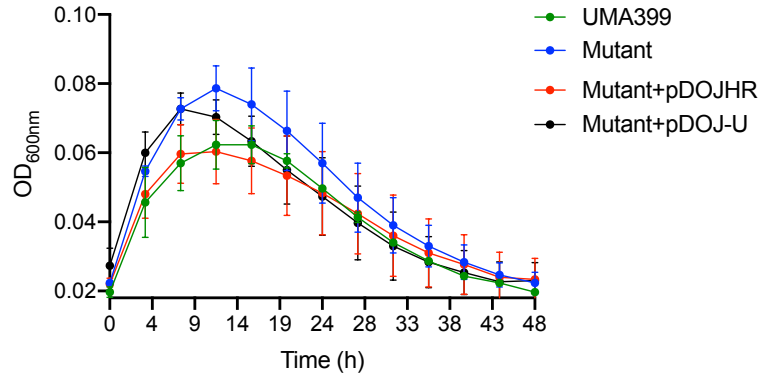


Figure A1. Growth phenotype of mutant, UMA399, Mutant + pDOJHR, and Mutant + pDOJ-U while growing in complex nitrogen.

Mutant + pDOJHR: mutant transferred with pDOJHR; Mutant + pDOJ-U: mutant transferred with pDOJ-U. UMA399 is the wild-type strain. The continuous growth curves display the optical density at 600 nm at each time point by mean \pm SD (standard deviation) from three individual biological replicates (n = 3).

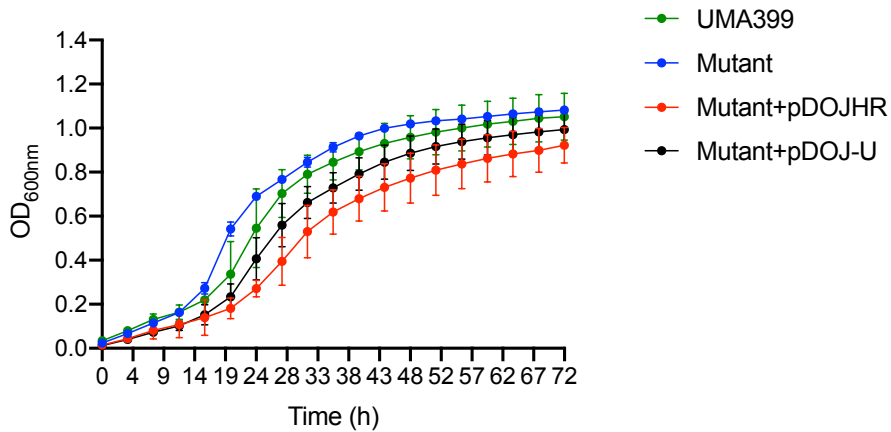


Figure A2. Growth phenotype of mutant, UMA399, Mutant + pDOJHR and Mutant + pDOJ-U while growing in negative control medium.

Mutant + pDOJHR: mutant transferred with pDOJHR; Mutant + pDOJ-U: mutant transferred with pDOJ-U. UMA399 is the wild-type strain. The continuous growth curves display the optical density at 600 nm at each time point by mean \pm SD (standard deviation) from three individual biological replicates (n = 3).

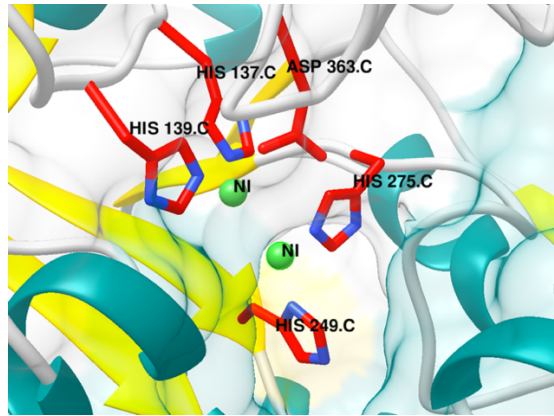


Figure A3. Predicted urease active site of UMA399 UreC

The Urease active site of UMA399 UreC. Ni^{2+} ions are shown in green; Amino acid residues in correlation with Ni^{2+} are shown in red carbon atoms, labeled with 3-letter code and number.

Figure A4. Construction of the UreC expression vector pSMT-U

The *ureC* fragment from wild-type and the mutant strain indicated in red was cloned in between the *Bam*HI and *Xho*I sites on the vector pSMT3, forming pSMT-U.

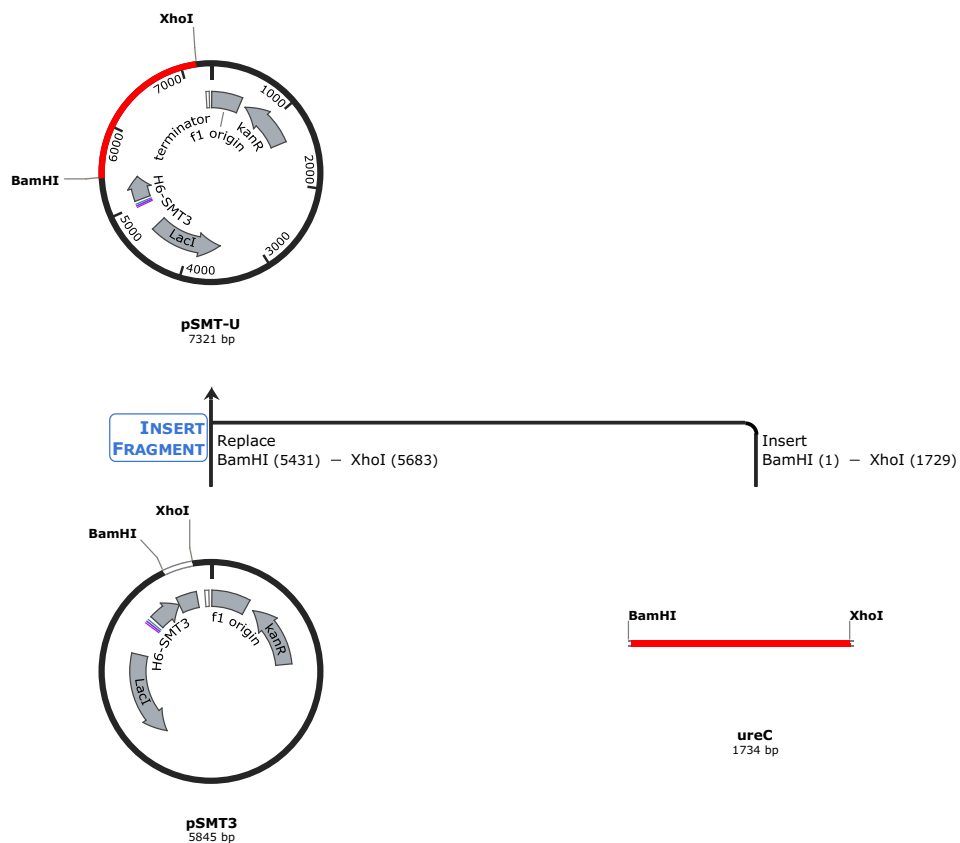


Figure A5. Construction of the UreC expression vector pDOJ-cysK-metB

The cystathionine beta-synthase and gamma-lyase indicated in red was cloned in between the *EcoRI* sites on the vector pDOJHR, forming pDOJ-cysK-metB

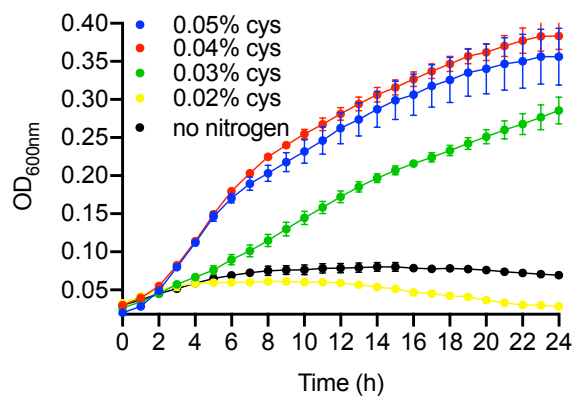
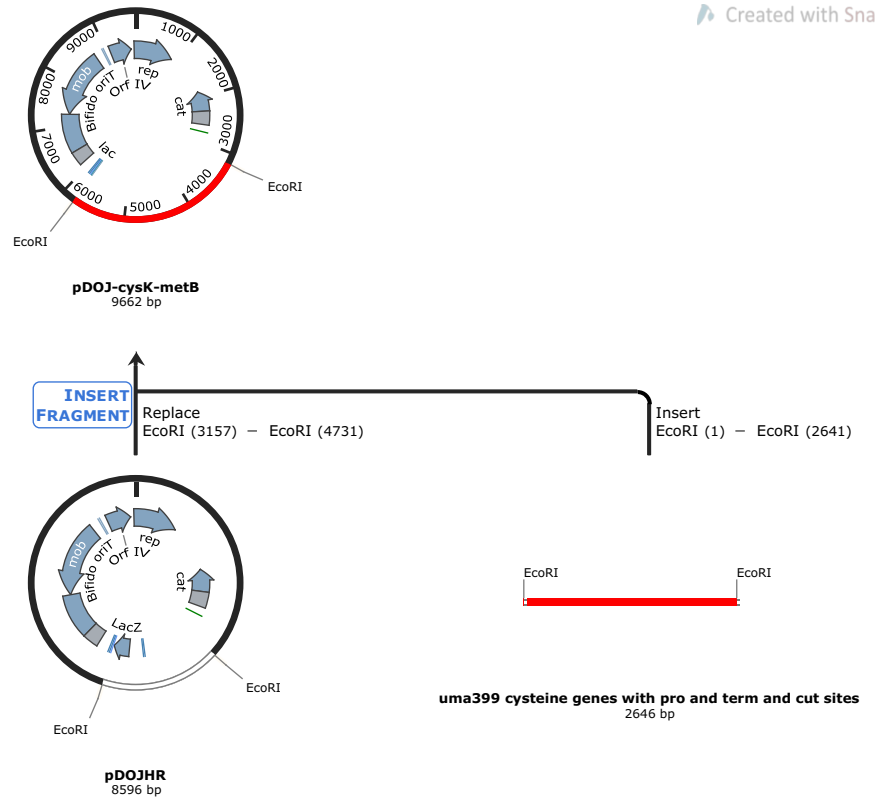


Figure A6. Growth phenotype of *B. boum* LMG10736 while growing in cysteine as the sole nitrogen source.

The continuous growth curves display the optical density at 600 nm at each time point by mean \pm SD (standard deviation) from three individual biological replicates ($n = 3$).

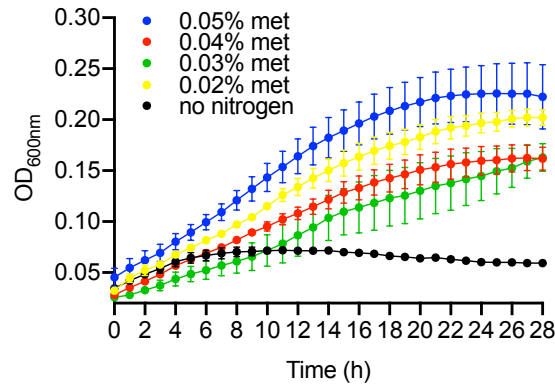


Figure A7. Growth phenotype of *B. boum* LMG10736 while growing in methionine as the sole nitrogen source.

The continuous growth curves display the optical density at 600 nm at each time point by mean \pm *SD* (standard deviation) from three individual biological replicates ($n = 3$).

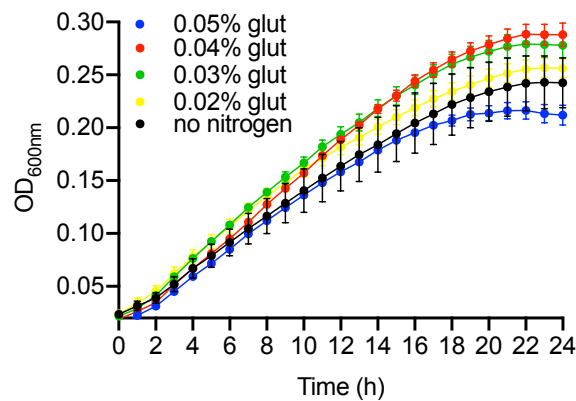


Figure A8. Growth phenotype of *B. boum* LMG10736 while growing in glutamine as the sole nitrogen source.

The continuous growth curves display the optical density at 600 nm at each time point by mean \pm *SD* (standard deviation) from three individual biological replicates ($n = 3$).

BIBLIOGRAPHY

1. Tanaka, M. and J. Nakayama, *Development of the gut microbiota in infancy and its impact on health in later life*. Allergology International, 2017. **66**(4): p. 515-522.
2. Rajilić-Stojanović, M. and W.M. de Vos, *The first 1000 cultured species of the human gastrointestinal microbiota*. FEMS microbiology reviews, 2014. **38**(5): p. 996-1047.
3. Kostic, A.D., et al., *The dynamics of the human infant gut microbiome in development and in progression toward type 1 diabetes*. Cell host & microbe, 2015. **17**(2): p. 260-273.
4. Karimi, G., et al., *The anti-obesity effects of Lactobacillus casei strain Shirota versus Orlistat on high fat diet-induced obese rats*. Food & nutrition research, 2015. **59**(1): p. 29273.
5. Quince, C., et al., *Extensive modulation of the fecal metagenome in children with Crohn's disease during exclusive enteral nutrition*. The American journal of gastroenterology, 2015. **110**(12): p. 1718.
6. Lee, Y.K., et al., *Proinflammatory T-cell responses to gut microbiota promote experimental autoimmune encephalomyelitis*. Proceedings of the National Academy of Sciences, 2011. **108**(Supplement 1): p. 4615-4622.
7. Lynch, S.V. and H.A. Boushey, *The microbiome and development of allergic disease*. Current opinion in allergy and clinical immunology, 2016. **16**(2): p. 165.
8. Schwabe, R.F. and C. Jobin, *The microbiome and cancer*. Nature Reviews Cancer, 2013. **13**(11): p. 800.
9. Wang, Y. and L.H. Kasper, *The role of microbiome in central nervous system disorders*. Brain, behavior, and immunity, 2014. **38**: p. 1-12.
10. Jandhyala, S.M., et al., *Role of the normal gut microbiota*. World journal of gastroenterology: WJG, 2015. **21**(29): p. 8787.

11. Oftedal, O.T., *The evolution of milk secretion and its ancient origins*. *Animal*, 2012. **6**(3): p. 355-368.
12. Carratù, B., et al., *Nitrogenous components of human milk: non-protein nitrogen, true protein and free amino acids*. *Food Chemistry*, 2003. **81**(3): p. 357-362.
13. Ballard, O. and A.L. Morrow, *Human milk composition: nutrients and bioactive factors*. *Pediatric Clinics*, 2013. **60**(1): p. 49-74.
14. Guglielmetti, S., et al., *Randomised clinical trial: Bifidobacterium bifidum MIMBb75 significantly alleviates irritable bowel syndrome and improves quality of life—a double-blind, placebo-controlled study*. *Alimentary pharmacology & therapeutics*, 2011. **33**(10): p. 1123-1132.
15. Turrone, F., et al., *Bifidobacterium bifidum PRL2010 modulates the host innate immune response*. *Appl. Environ. Microbiol.*, 2014. **80**(2): p. 730-740.
16. Zanotti, I., et al., *Evidence for cholesterol-lowering activity by Bifidobacterium bifidum PRL2010 through gut microbiota modulation*. *Applied microbiology and biotechnology*, 2015. **99**(16): p. 6813-6829.
17. Ku, S., et al., *Review on bifidobacterium bifidum bgn4: Functionality and nutraceutical applications as a probiotic microorganism*. *International journal of molecular sciences*, 2016. **17**(9): p. 1544.
18. Murray, N.E., *Immigration control of DNA in bacteria: self versus non-self*. *Microbiology*, 2002. **148**(1): p. 3-20.
19. Tock, M.R. and D.T. Dryden, *The biology of restriction and anti-restriction*. *Current opinion in microbiology*, 2005. **8**(4): p. 466-472.
20. Roberts, R.J., et al., *A nomenclature for restriction enzymes, DNA methyltransferases, homing endonucleases and their genes*. *Nucleic acids research*, 2003. **31**(7): p. 1805-1812.
21. Kobayashi, I., *Behavior of restriction–modification systems as selfish mobile elements and their impact on genome evolution*. *Nucleic acids research*, 2001. **29**(18): p. 3742-3756.

22. Pingoud, A., et al., *Type II restriction endonucleases: structure and mechanism*. Cellular and molecular life sciences, 2005. **62**(6): p. 685.
23. Roberts, R., et al., *REBASE—restriction enzymes and methylases*. 2003.
24. Rossi, M., et al., *Characterization of the plasmid pMB1 from Bifidobacterium longum and its use for shuttle vector construction*. Research in microbiology, 1996. **147**(3): p. 133-143.
25. Bottacini, F., et al., *Comparative genome and methylome analysis reveals restriction/modification system diversity in the gut commensal Bifidobacterium breve*. Nucleic acids research, 2017. **46**(4): p. 1860-1877.
26. Lee, J.-H. and D.J. O’Sullivan, *Sequence analysis of two cryptic plasmids from Bifidobacterium longum DJO10A and construction of a shuttle cloning vector*. Applied and environmental microbiology, 2006. **72**(1): p. 527-535.
27. Yasui, K., et al., *Improvement of bacterial transformation efficiency using plasmid artificial modification*. Nucleic acids research, 2008. **37**(1): p. e3-e3.
28. O’Connell Motherway, M., et al., *Overcoming the restriction barrier to plasmid transformation and targeted mutagenesis in Bifidobacterium breve UCC2003*. Microb Biotechnol, 2009. **2**(3): p. 321-32.
29. Serafini, F., et al., *An efficient and reproducible method for transformation of genetically recalcitrant bifidobacteria*. FEMS microbiology letters, 2012. **333**(2): p. 146-152.
30. Sun, Z., et al., *Accessing the inaccessible: molecular tools for bifidobacteria*. Appl. Environ. Microbiol., 2012. **78**(15): p. 5035-5042.
31. Guglielmetti, S., B. Mayo, and P. Álvarez-Martín, *Mobilome and genetic modification of bifidobacteria*. Beneficial microbes, 2012. **4**(2): p. 143-166.
32. Bottacini, F., et al., *Comparative genome and methylome analysis reveals restriction/modification system diversity in the gut commensal Bifidobacterium breve*. Nucleic Acids Research, 2018. **46**(4): p. 1860-1877.

33. Park, M.J., M.S. Park, and G.E. Ji, *Improvement of electroporation-mediated transformation efficiency for a Bifidobacterium strain to a reproducibly high level*. Journal of microbiological methods, 2019. **159**: p. 112-119.
34. Fukiya, S., M. Sakanaka, and A. Yokota, *Genetic Manipulation and Gene Modification Technologies in Bifidobacteria*, in *The Bifidobacteria and Related Organisms*. 2018, Elsevier. p. 243-259.
35. Brancaccio, V.F., D.S. Zhurina, and C.U. Riedel, *Tough nuts to crack: site-directed mutagenesis of bifidobacteria remains a challenge*. Bioengineered, 2013. **4**(4): p. 197-202.
36. Schiavi, E., et al., *The surface-associated exopolysaccharide of Bifidobacterium longum 35624 plays an essential role in dampening host proinflammatory responses and repressing local TH17 responses*. Appl. Environ. Microbiol., 2016. **82**(24): p. 7185-7196.
37. Grimm, V., et al., *Expression of fluorescent proteins in bifidobacteria for analysis of host-microbe interactions*. Appl. Environ. Microbiol., 2014. **80**(9): p. 2842-2850.
38. Cronin, M., et al., *Development of a luciferase-based reporter system to monitor Bifidobacterium breve UCC2003 persistence in mice*. BMC microbiology, 2008. **8**(1): p. 161.
39. Sakanaka, M., et al., *Functional analysis of bifidobacterial promoters in Bifidobacterium longum and Escherichia coli using the α -galactosidase gene as a reporter*. Journal of bioscience and bioengineering, 2014. **118**(5): p. 489-495.
40. Yu, Z., et al., *Bifidobacterium as an oral delivery carrier of interleukin-12 for the treatment of Coxsackie virus B3-induced myocarditis in the Balb/c mice*. International immunopharmacology, 2012. **12**(1): p. 125-130.
41. Ruiz, L., et al., *Controlled gene expression in bifidobacteria by use of a bile-responsive element*. Appl. Environ. Microbiol., 2012. **78**(2): p. 581-585.
42. Sun, Z., et al., *Experimental determination and characterization of the gap promoter of Bifidobacterium bifidum S17*. Bioengineered, 2014. **5**(6): p. 371-377.

43. He, J., K. Sakaguchi, and T. Suzuki, *Determination of the ribosome-binding sequence and spacer length between binding site and initiation codon for efficient protein expression in Bifidobacterium longum 105-A*. Journal of bioscience and bioengineering, 2012. **113**(4): p. 442-444.
44. Griffiths, A.J., et al., *An introduction to genetic analysis*. 2005: Macmillan.
45. O'Connell Motherway, M., et al., *Overcoming the restriction barrier to plasmid transformation and targeted mutagenesis in Bifidobacterium breve UCC2003*. Microbial biotechnology, 2009. **2**(3): p. 321-332.
46. Sakaguchi, K., et al., *A targeted gene knockout method using a newly constructed temperature-sensitive plasmid mediated homologous recombination in Bifidobacterium longum*. Applied microbiology and biotechnology, 2012. **95**(2): p. 499-509.
47. Fukuda, S., et al., *Bifidobacteria can protect from enteropathogenic infection through production of acetate*. Nature, 2011. **469**(7331): p. 543.
48. Sakurama, H., et al., *Lacto-N-biosidase encoded by a novel gene of Bifidobacterium longum subspecies longum shows unique substrate specificity and requires a designated chaperone for its active expression*. Journal of Biological Chemistry, 2013. **288**(35): p. 25194-25206.
49. O'Callaghan, A., et al., *Pangenome analysis of Bifidobacterium longum and site-directed mutagenesis through by-pass of restriction-modification systems*. BMC genomics, 2015. **16**(1): p. 832.
50. Arigoni, F., *Genetic remodeling in Bifidobacterium*. International Patent, WO 2008/019886A1, 2008.
51. Hidalgo-Cantabrana, C., et al., *A single mutation in the gene responsible for the mucoid phenotype of Bifidobacterium animalis subsp. lactis confers surface and functional characteristics*. Appl. Environ. Microbiol., 2015. **81**(23): p. 7960-7968.
52. O'Connell, K.J., et al., *Identification and characterization of an oleate hydratase-encoding gene from Bifidobacterium breve*. Bioengineered, 2013. **4**(5): p. 313-321.

53. Egan, M., et al., *Glycosulfatase-encoding gene cluster in Bifidobacterium breve UCC2003*. Appl. Environ. Microbiol., 2016. **82**(22): p. 6611-6623.
54. O'Connell, K.J., et al., *Transcription of two adjacent carbohydrate utilization gene clusters in Bifidobacterium breve UCC2003 is controlled by LacI-and repressor open reading frame kinase (ROK)-type regulators*. Appl. Environ. Microbiol., 2014. **80**(12): p. 3604-3614.
55. Motherway, M.O.C., et al., *Characterization of ApuB, an extracellular type II amylopullulanase from Bifidobacterium breve UCC2003*. Appl. Environ. Microbiol., 2008. **74**(20): p. 6271-6279.
56. Pokusaeva, K., et al., *Ribose utilization by the human commensal Bifidobacterium breve UCC2003*. Microbial biotechnology, 2010. **3**(3): p. 311-323.
57. Matsuki, T., et al., *A key genetic factor for fucosyllactose utilization affects infant gut microbiota development*. Nature communications, 2016. **7**: p. 11939.
58. Bottacini, F., et al., *Discovery of a conjugative megaplasmid in Bifidobacterium breve*. Appl. Environ. Microbiol., 2015. **81**(1): p. 166-176.
59. Bottacini, F., et al., *Comparative genomics of the Bifidobacterium breve taxon*. BMC genomics, 2014. **15**(1): p. 170.
60. Moresco, E.M.Y., X. Li, and B. Beutler, *Going forward with genetics: recent technological advances and forward genetics in mice*. The American journal of pathology, 2013. **182**(5): p. 1462-1473.
61. Faivre, D. and J. Baumgartner, *The combination of random mutagenesis and sequencing highlight the role of unexpected genes in an intractable organism*. PLoS genetics, 2015. **11**(1): p. e1004895.
62. Mohd-Yusoff, N.F., et al., *Scanning the effects of ethyl methanesulfonate on the whole genome of Lotus japonicus using second-generation sequencing analysis*. G3: Genes, Genomes, Genetics, 2015. **5**(4): p. 559-567.
63. Ibrahim, S.A. and D.J. O'Sullivan, *Use of chemical mutagenesis for the isolation of food grade β -galactosidase overproducing mutants of bifidobacteria, lactobacilli and Streptococcus thermophilus*. Journal of dairy science, 2000. **83**(5): p. 923-930.

64. Keung, H.Y., et al., *Mechanistic study of utilization of water-insoluble Saccharomyces cerevisiae glucans by Bifidobacterium breve strain JCM1192*. Appl. Environ. Microbiol., 2017. **83**(7): p. e03442-16.
65. Ruiz, L., et al., *Transposon mutagenesis in Bifidobacterium breve: construction and characterization of a Tn5 transposon mutant library for Bifidobacterium breve UCC2003*. PLoS One, 2013. **8**(5): p. e64699.
66. Muñoz-López, M. and J.L. García-Pérez, *DNA transposons: nature and applications in genomics*. Current genomics, 2010. **11**(2): p. 115-128.
67. Jacobs, M.A., et al., *Comprehensive transposon mutant library of Pseudomonas aeruginosa*. Proceedings of the National Academy of Sciences, 2003. **100**(24): p. 14339-14344.
68. Hsu, P.D., E.S. Lander, and F. Zhang, *Development and applications of CRISPR-Cas9 for genome engineering*. Cell, 2014. **157**(6): p. 1262-1278.
69. Cui, L. and D. Bikard, *Consequences of Cas9 cleavage in the chromosome of Escherichia coli*. Nucleic acids research, 2016. **44**(9): p. 4243-4251.
70. Oh, J.-H. and J.-P. van Pijkeren, *CRISPR–Cas9-assisted recombineering in Lactobacillus reuteri*. Nucleic acids research, 2014. **42**(17): p. e131-e131.
71. van Pijkeren, J.P. and R.A. Britton, *High efficiency recombineering in lactic acid bacteria*. Nucleic Acids Res, 2012. **40**(10): p. e76.
72. Mary, O., et al., *Identification of restriction-modification systems of Bifidobacterium animalis subsp. lactis CNCM I-2494 by SMRT sequencing and associated methylome analysis*. PloS one, 2014. **9**(4): p. e94875.
73. Underwood, M.A., et al., *Bifidobacterium longum subspecies infantis: champion colonizer of the infant gut*. Pediatr Res, 2015. **77**(1-2): p. 229-35.
74. Sela, D.A. and D.A. Mills, *Nursing our microbiota: molecular linkages between bifidobacteria and milk oligosaccharides*. Trends in microbiology, 2010. **18**(7): p. 298-307.

75. Sela, D.A., *Bifidobacterial utilization of human milk oligosaccharides*. Int J Food Microbiol, 2011. **149**(1): p. 58-64.
76. Donovan, S.M. and B. Lonnerdal, *Non-protein nitrogen and true protein in infant formulas*. Acta Paediatr Scand, 1989. **78**(4): p. 497-504.
77. Sela, D.A., et al., *The genome sequence of Bifidobacterium longum subsp. infantis reveals adaptations for milk utilization within the infant microbiome*. Proc Natl Acad Sci U S A, 2008. **105**(48): p. 18964-9.
78. Kwak, M.J., et al., *Evolutionary architecture of the infant-adapted group of Bifidobacterium species associated with the probiotic function*. Syst Appl Microbiol, 2016. **39**(7): p. 429-439.
79. Marshall, B.J., et al., *Urea protects Helicobacter (Campylobacter) pylori from the bactericidal effect of acid*. Gastroenterology, 1990. **99**(3): p. 697-702.
80. Matteuzzi, D. and F. Crociani, *Urease production and DNA-homology in the species Bifidobacterium suis*. Archiv für Mikrobiologie, 1973. **94**(1): p. 93-95.
81. Suzuki, K., et al., *Urease-producing species of intestinal anaerobes and their activities*. Applied and Environmental Microbiology, 1979. **37**(3): p. 379-382.
82. Crociani, F. and D. Matteuzzi, *Urease activity in the genus Bifidobacterium*. Ann Microbiol (Paris), 1982. **133**(3): p. 417-23.
83. Read, W., et al., *Studies with 15 N-labeled ammonia and urea in the malnourished child*. The Journal of clinical investigation, 1969. **48**(6): p. 1143-1149.
84. Heine, W., C. Mohr, and K.D. Wutzke, *Host-microflora correlations in infant nutrition*. Prog Food Nutr Sci, 1992. **16**(2): p. 181-97.
85. Fuller, M.F. and P.J. Reeds, *Nitrogen cycling in the gut*. Annu Rev Nutr, 1998. **18**: p. 385-411.
86. Millward, D.J., et al., *The transfer of 15N from urea to lysine in the human infant*. Br J Nutr, 2000. **83**(5): p. 505-12.

87. Monnet, C., et al., *Selection and properties of Streptococcus thermophilus mutants deficient in urease*. J Dairy Sci, 2004. **87**(6): p. 1634-40.
88. Veltri, D., M.M. Wight, and J.A. Crouch, *SimpleSynteny: a web-based tool for visualization of microsynteny across multiple species*. Nucleic acids research, 2016. **44**(W1): p. W41-W45.
89. Weatherburn, M.W., *Phenol-Hypochlorite Reaction for Determination of Ammonia*. Analytical Chemistry, 1967. **39**(8): p. 971-+.
90. Herbst, R.W., et al., *Communication between the zinc and nickel sites in dimeric HypA: metal recognition and pH sensing*. Journal of the American Chemical Society, 2010. **132**(30): p. 10338-10351.
91. Niesen, F.H., H. Berglund, and M. Vedadi, *The use of differential scanning fluorimetry to detect ligand interactions that promote protein stability*. Nature protocols, 2007. **2**(9): p. 2212.
92. Bottacini, F., et al., *Comparative genome and methylome analysis reveals restriction/modification system diversity in the gut commensal Bifidobacterium breve*. Nucleic Acids Res, 2018. **46**(4): p. 1860-1877.
93. Quan, L., Q. Lv, and Y. Zhang, *STRUM: structure-based prediction of protein stability changes upon single-point mutation*. Bioinformatics, 2016. **32**(19): p. 2936-2946.
94. Waterhouse, A., et al., *SWISS-MODEL: homology modelling of protein structures and complexes*. Nucleic acids research, 2018.
95. Pettersen, E.F., et al., *UCSF Chimera—a visualization system for exploratory research and analysis*. Journal of computational chemistry, 2004. **25**(13): p. 1605-1612.
96. Katoh, K., J. Rozewicki, and K.D. Yamada, *MAFFT online service: multiple sequence alignment, interactive sequence choice and visualization*. Briefings in bioinformatics, 2017.
97. Guindon, S., et al., *New algorithms and methods to estimate maximum-likelihood phylogenies: assessing the performance of PhyML 3.0*. Systematic biology, 2010. **59**(3): p. 307-321.

98. Lefort, V., J.-E. Longueville, and O. Gascuel, *SMS: smart model selection in PhyML*. *Molecular biology and evolution*, 2017. **34**(9): p. 2422-2424.
99. Rambaut, A., *FigTree-version 1.4. 3, a graphical viewer of phylogenetic trees*. 2017.
100. Mohd-Yusoff, N.F., et al., *Scanning the Effects of Ethyl Methanesulfonate on the Whole Genome of Lotus japonicus Using Second-Generation Sequencing Analysis*. *G3-Genes Genomes Genetics*, 2015. **5**(4): p. 559-567.
101. Donangelo, C. and N. Trugo, *LACTATION| Human Milk: Composition and Nutritional Value*. 2003.
102. Krachler, M., et al., *Concentrations of selected trace elements in human milk and in infant formulas determined by magnetic sector field inductively coupled plasma-mass spectrometry*. *Biological Trace Element Research*, 2000. **76**(2): p. 97-112.
103. Mohd-Taufek, N., et al., *The simultaneous analysis of eight essential trace elements in human milk by ICP-MS*. *Food Analytical Methods*, 2016. **9**(7): p. 2068-2075.
104. Aquilio, E., et al., *Trace element content in human milk during lactation of preterm newborns*. *Biological trace element research*, 1996. **51**(1): p. 63-70.
105. Gunshin, H., et al., *Trace elements in human milk, cow's milk, and infant formula*. *Agricultural and Biological Chemistry*, 1985. **49**(1): p. 21-26.
106. Lensmire, J.M. and N.D. Hammer, *Nutrient sulfur acquisition strategies employed by bacterial pathogens*. *Current opinion in microbiology*, 2019. **47**: p. 52-58.
107. Qian, Y., W.J. Borowski, and W.D. Calhoon, *Intracellular granule formation in response to oxidative stress in Bifidobacterium*. *International journal of food microbiology*, 2011. **145**(1): p. 320-325.
108. Zhang, Z., et al., *Amino acid profiles in term and preterm human milk through lactation: a systematic review*. *Nutrients*, 2013. **5**(12): p. 4800-4821.

109. Tomasova, L., P. Konopelski, and M. Ufnal, *Gut Bacteria and Hydrogen Sulfide: The New Old Players in Circulatory System Homeostasis*. *Molecules*, 2016. **21**(11).
110. Bogicevic, B., et al., *CysK from Lactobacillus casei encodes a protein with O-acetylserine sulphydrylase and cysteine desulfurization activity*. *Applied microbiology and biotechnology*, 2012. **94**(5): p. 1209-1220.
111. VEDA, M., et al., *Establishment of a defined minimal medium and isolation of auxotrophic mutants for Bifidobacterium bifidum es 5*. *The Journal of General and Applied Microbiology*, 1983. **29**(2): p. 103-114.
112. Milani, C., et al., *Genomic encyclopedia of type strains of the genus Bifidobacterium*. *Appl. Environ. Microbiol.*, 2014. **80**(20): p. 6290-6302.
113. Ferrario, C., et al., *Exploring amino acid auxotrophy in Bifidobacterium bifidum PRL2010*. *Frontiers in microbiology*, 2015. **6**: p. 1331.
114. Bogicevic, B., et al., *Cysteine biosynthesis in Lactobacillus casei: identification and characterization of a serine acetyltransferase*. *FEMS microbiology letters*, 2016. **363**(4): p. fnw012.
115. Lee, J.-H. and D.J. O'Sullivan, *Genomic insights into bifidobacteria*. *Microbiol. Mol. Biol. Rev.*, 2010. **74**(3): p. 378-416.
116. Karp, P.D., et al., *Pathway Tools version 13.0: integrated software for pathway/genome informatics and systems biology*. *Briefings in bioinformatics*, 2009. **11**(1): p. 40-79.
117. Ferrario, C., et al., *Exploring Amino Acid Auxotrophy in Bifidobacterium bifidum PRL2010*. *Front Microbiol*, 2015. **6**: p. 1331.
118. Rozen, S. and H. Skaletsky, *Primer3 on the WWW for general users and for biologist programmers*, in *Bioinformatics methods and protocols*. 2000, Springer. p. 365-386.

119. Livak, K.J. and T.D. Schmittgen, *Analysis of relative gene expression data using real-time quantitative PCR and the 2⁻ ΔΔCT method*. *methods*, 2001. **25**(4): p. 402-408.
120. Gaora, P.O., *Expression of genes in mycobacteria*. *Methods Mol Biol*, 1998. **101**: p. 261-73.